New Craniodental Remains of the Quaternary Jamaican Monkey Xenothrix mcgregori (Xenotrichini, Callicebinae, Pitheciidae), with a Reconsideration of the Aotus Hypothesis 1

Authors: MACPHEE, R.D.E., and HOROVITZ, INÉS

Source: American Museum Novitates, 2004(3434) : 1-51

Published By: American Museum of Natural History

URL: https://doi.org/10.1206/0003-0082(2004)434<0001:NCROTQ>2.0.CO;2

AMERICAN MUSEUM
Novitates

PUBLISHED BY THE AMERICAN MUSEUM OF NATURAL HISTORY
CENTRAL PARK WEST AT 79TH STREET, NEW YORK, NY 10024
Number 3434, 51 pp., 17 figures, 13 tables May 14, 2004

New Craniodental Remains of the Quaternary Jamaican Monkey *Xenothrix mcgregori* (Xenotrichini, Callicebinae, Pitheciidae), with a Reconsideration of the *Aotus* Hypothesis[1]

R.D.E. MACPHEE[2] AND INÉS HOROVITZ[3]

ABSTRACT

The Jamaican monkey *Xenothrix mcgregori* is one of several extinct endemic platyrrhines known from the late Quaternary of the Greater Antilles. Until recently, the hypodigm of *Xenothrix* was limited to the holotype partial mandible and a handful of tentatively referred postcranial elements. Here we describe several additional fossils attributable to *Xenothrix*, including the first cranial remains, all of which were recovered in cave deposits in the Jackson's Bay region of southern Jamaica. In addition to a partial face from Lloyd's Cave and a maxillary fragment of a different individual from the same site, the craniodental collection includes two incomplete mandibles with poorly preserved cheekteeth from nearby Skeleton Cave. The new specimens confirm a distinctive derived feature of *Xenothrix*, i.e., reduced dental formula in both jaws (2/2 1/1 3/3 2/2). Although no examples of the maxillary canine are yet known, its alveolus is notably small. Similarly, although the upper face of *Xenothrix* is also unknown, it is clear that the maxillary sinuses were large enough to encroach significantly on the bases of the zygomatic processes. The nasal fossa is also very large and wider than the palate at the latter's widest point. A similar condition is seen in the extinct Cuban monkey *Paralouatta varonai*.

Xenothrix continues to generate disputes among platyrrhine specialists because its unusual

[1] Contribution 7 to the series ''Origin of the Antillean Land Mammal Fauna''.

[2] Division of Vertebrate Zoology (Mammalogy), American Museum of Natural History. e-mail: macphee@amnh.org

[3] Department of Organismal Biology, Ecology and Evolution, University of California, Los Angeles; Research Associate, Department of Vertebrate Paleontology, American Museum of Natural History. e-mail: horovitz@obee.ucla.edu

 ISSN 0003-0082

combination of apomorphies complicates its systematic placement. Rosenberger's recent ''*Aotus* hypothesis'' stipulates that *Xenothrix* is a close relative of the living owl monkey (*Aotus*) and is not a pitheciid sensu stricto. Two fundamental characters used to support this hypothesis—hypertrophied orbits and enlarged central incisors—can be shown to be inapplicable or uninterpretable on the basis of the existing hypodigm of *Xenothrix*. The new craniodental evidence confirms our earlier cladistic results showing that the Antillean monkeys (*Xenothrix mcgregori, Paralouatta varonai*, and *Antillothrix bernensis*) are closely related and that *Callicebus* is their closest joint extant mainland relative. This may be expressed systematically by placing the three Antillean taxa in **Xenotrichini,** new tribe, adjacent to Callicebini, their sister-group within subfamily Callicebinae (Pitheciidae).

RESUMEN

El mono jamaiquino *Xenothrix mcgregori* es una de las varias especies endémicas de monos platirrinos extintos conocidos del Cuaternario tardío de las Antillas Mayores. Hasta recientemente, el hipodigma de *Xenothrix* estaba limitado al holotipo, que consiste en una mandíbula, y a unos pocos elementos postcraneanos tentativamente referidos a esta especie. Describimos aquí varios restos fósiles adicionales atribuibles a *Xenothrix* incluyendo los primeros restos craneanos, todos los cuales fueron encontrados en depósitos cavernarios en la zona de la bahía de Jackson en el sur de Jamaica. Además de un resto facial parcial de la cueva de Lloyd y un fragmento de maxilar de otro individuo de la misma localidad, la colección de restos craneodentales incluye dos mandíbulas incompletas provenientes de la cueva cercana de Skeleton, con premolares y molares pobremente preservados. Los especímenes nuevos confirman un carácter derivado distintivo de *Xenothrix*, i.e., una fórmula dentaria maxilar y mandibular reducida (2/2 1/1 3/3 2/2). A pesar de que no se conoce ningún ejemplar de canino superior, el alvéolo correspondiente es notablemente pequeño. Asimismo, a pesar de que la parte superior de la cara no se conoce, está claro que los senos maxilares eran lo suficientemente grandes como para invadir las bases de los procesos cigomáticos en forma significativa. La fosa nasal era muy grande también y más ancha que el paladar en su punto más ancho. Se puede apreciar una condición similar en el mono cubano extinto *Paralouatta varonai*.

Xenothrix continúa generando discusiones entre los especialistas en platirrinos porque su inusual combinación de apomorfías complica su posición sistemática. La ''hipótesis *Aotus*'' recientemente propuesta por Rosenberger estipula que *Xenothrix* está cercanamente emparentado con el mono almiquí (*Aotus*) más que un pitecido en sentido estricto. Dos caracteres fundamentales usados para apoyar esta hipótesis—órbitas hipertrofiadas e incisivos centrales grandes—no se pueden codificar o no pueden ser interpretados en base al hipodigma existente de *Xenothrix*. La nueva evidencia craneodental confirma nuestros resultados cladísticos anteriores indicando que los monos antillanos (*Xenothrix mcgregori, Paralouatta varonai*, and *Antillothrix bernensis*), están cercanamente emparentados entre sí y que *Callicebus* es su pariente más cercano en tierra firme. Esto se puede expresar en forma sistemática ubicando a los tres taxones antillanos en **Xenotrichini,** tribu nueva, adyacente a Callicebini, su grupo hermano dentro de la subfamilia Callicebinae (Pitheciidae).

INTRODUCTION

Until recently, virtually nothing was known about *Xenothrix mcgregori* Williams and Koopman (1952) beyond the bare facts that this extinct platyrrhine monkey lived in Jamaica during the latest part of the Quaternary and possessed unusual dental features. For several decades after its initial description, the only item in the *Xenothrix* hypodigm was the holotype itself, a partial mandible chiefly remarkable for its callitrichine-like dental formula (/2 /1 /3 /2). In their original report, Williams and Koopman (1952) briefly noted the existence of poorly preserved but rather primatelike postcranial remains in the same bone collection from Long Mile Cave that yielded the type jaw (for historical details, see MacPhee, 1996). However, they refrained from describing this material on the ground that its allocation would be uncertain. Forty years later, the Long Mile postcranials were finally described and mostly allocated to *Xenothrix*, al-

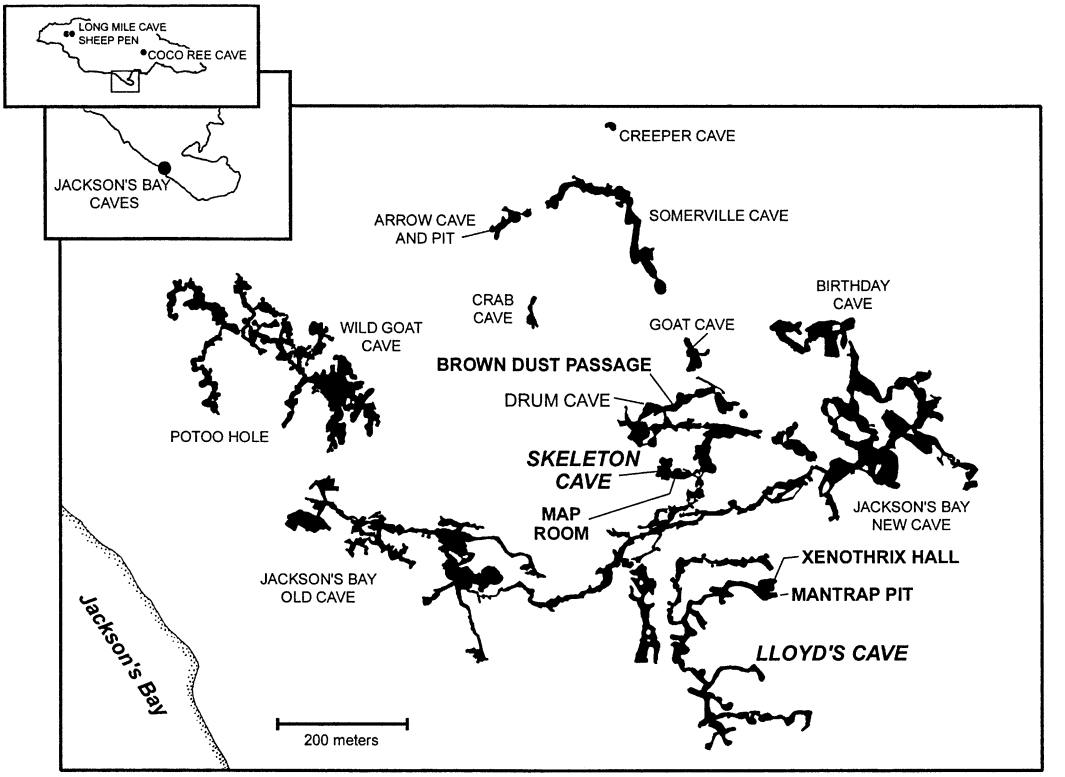

Fig. 1. Map of Jamaica and *Xenothrix* localities: Caves on the eastern flank of Portland Ridge near Jackson's Bay in southern Clarendon Parish have produced several new specimens of *Xenothrix mcgregori* (plans after Fincham, 1997; see also table 1). Three other localities (Long Mile Cave, Sheep Pen, and Coco Ree Cave) elsewhere on the island are also known as ''primate caves'', although Long Mile is the only one that has definitely yielded *Xenothrix* material.

though not without a question mark in some cases (MacPhee and Fleagle, 1991).

In the 1990s, joint expeditions of the American Museum of Natural History and Claremont-McKenna College recovered several cranial and postcranial specimens referable to *Xenothrix mcgregori* from a number of cave localities in the Jackson's Bay area on the island's south coast (figs. 1, 2). The hypodigm of this very rare primate now stands at 17 specimens, no two of which are known to be from the same individual. In this paper we describe two new partial mandibles and the first cranial remains attributable to this species (table 1), including a partial face (AMNHM 268006) preserving the entire palate and most cheekteeth in situ, the floor of the nasal fossa, and portions of the orbits and nasal septum; and a left maxillary fragment (AMNHM 268007) with PM3–M2 still in place. These specimens are abundantly illustrated in figures 3–6 and 9–11.

Several more recent expeditions to the Jackson's Bay caves, including those of other teams, have failed to turn up additional fossils of the Jamaican monkey. This is not surprising. Most living primates have little or nothing to do with caves as such, and *Xenothrix* was probably no exception: individuals who accidentally fell in probably had little trouble getting out—most of the time. None of the craniodental fossils so far recovered shows any appreciable degree of mineralization, although a thin incrustation of calcium carbonate occurs on some bones. All specimens are presumably latest Pleistocene to late Holocene (see below), although somewhat greater ages have been reported for possible primate fossils found elsewhere on the island (cf. Ford and Morgan, 1988).

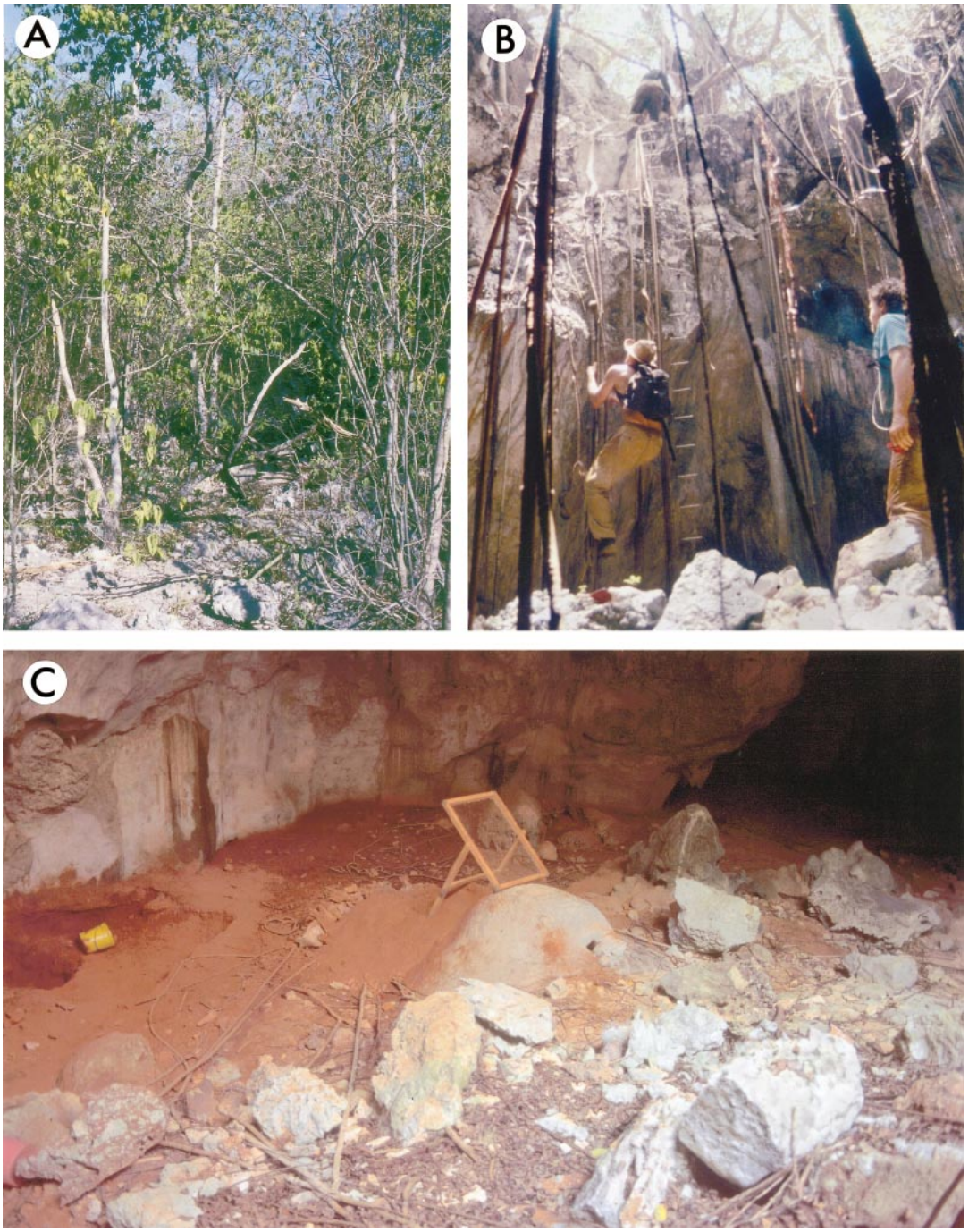

Fig. 2. Jackson's Bay caves and environment: (**A**) Typical Caribbean dry forest formation on limestone substrate, en route to Drum Cave. (**B**) Mantrap Pit entrance to Lloyd's Cave: skylight or pitfall entrances, acting as natural traps, are common in Jackson's Bay caves. (**C**) Inside Lloyd's Cave near Mantrap Pit: the new partial face and maxillary fragment of *Xenothrix* (AMNHM 268006, 268007) were recovered in surface debris just inside the chamber (Xenothrix Hall) that opens along the north wall (see fig. 1 and Fincham, 1997: 230).

TABLE 1
***Xenothrix mcgregori*: Cranial Remains**

AMNHM no.	Element	Site[a]	Description
148198[b]	Mandible (L)	Long Mile Cave	Ramus, m1–m2
268001	Mandible (L)	Skeleton Cave	Ramus, pm3–m2
268004	Mandible (L)	Skeleton Cave	Ramus, m1–m2
268006	Skull	Lloyd's Cave	Partial face, PM4–M2
268007	Maxilla (L)	Lloyd's Cave	PM3–M2

[a]Localities are identified under these same names in Fincham's (1997) catalog, to which the reader is referred for further details.
[b]Holotype.

Preliminary notes on some of these specimens have already been published (Horovitz et al., 1997; MacPhee, 1997; MacPhee and Horovitz, 2002). The purpose of this paper is to synthesize and extend these descriptions and to respond to a recent reevaluation of the phylogenetic position of *Xenothrix* and its allies. Descriptions of the new postcranial finds, which amplify and corroborate conclusions previously reached by MacPhee and Fleagle (1991), will be presented elsewhere.

The varied opinions regarding the phylogenetic affinities of *Xenothrix mcgregori* and its relatives have been summarized on several occasions (e.g., Rosenberger, 1977; Ford, 1986a, 1990; MacPhee, 1996; Horovitz, 1999; Horovitz and MacPhee, 1999; MacPhee and Horovitz, 2002). Williams and Koopman (1952) classified the Jamaican monkey rather vaguely as ''cebid *incertae sedis*'', essentially equivalent to ''non-callitrichid platyrrhine'' in their systematics. Hershkovitz (1977) thought that *Xenothrix* was not very closely related to any existing lineage and placed it in its own family, Xenotrichidae, a solution briefly endorsed by MacPhee and Fleagle (1991). Ford (1986a, 1986b, 1990) has remained persistently agnostic about the position of *Xenothrix*, although she regarded it as possibly cebid in affinity. More radically, she theorized on other grounds that the Greater Antilles had been colonized by callitrichines as well, basing her argument on a relatively large primate tibia from Samaná Bay, western Hispaniola (now included within the hypodigm of *Antillothrix bernensis* by MacPhee et al. [1995]) and unusual femoral specimens from the sites of Coco Ree Cave and Sheep Pen, central Jamaica (Ford and Morgan, 1986, 1988). MacPhee and Fleagle (1991) concluded that the femora were of the wrong size and shape to belong to *Xenothrix*, for which they had a better candidate. Since then no additional fossils attributable to the taxon represented by the Coco Ree and Sheep Pen femora have been recognized, and its affinities remain moot (but see also MacPhee and Flemming, 2003).

Rosenberger (e.g., 1977, 2002; Rosenberger et al., 1990) has argued on a number of occasions that the Jamaican monkey is phyletically closest to titi monkeys (*Callicebus*) among living platyrrhines. In modern systematic treatments titis are usually placed close to sakis and uakaris in Pitheciidae.[4] Rosenberger (e.g., 1977) has also remarked on certain resemblances between *Xenothrix* and other platyrrhines (particularly *Aotus*), although until recently without drawing any particular phylogenetic implications therefrom. Features originally cited by Rosenberger (1977; Rosenberger et al., 1990) in favor of an association between *Xenothrix* and Pitheciidae (in our sense) include: presence of an offset entoconid and a posttalonid extension, together with low cusp relief, short cristid obliqua, and differentiated postprotocristid. In favor of a specific association with *Callicebus* are: small canine socket, posteriorly broadening premolar alveoli, parabolic dental arcade, and jaw that markedly deepens

[4] In this paper Pitheciinae (saki and uakari monkeys: *Pithecia*, *Chiropotes*, and *Cacajao*) and Callicebinae (titi monkey: *Callicebus*) are grouped as family Pitheciidae, superfamily Ateloidea. Although there is some overlap in body size among pitheciid taxa, species of *Chiropotes* and *Cacajao* can be considered ''large-bodied''; those of *Pithecia* are ''mid-sized'', and those of *Callicebus* ''small-bodied''.

posteriorly. Rosenberger also correctly inferred from the morphology and wear of the ectoflexid that *Xenothrix* must have had a relatively well developed paracone and metacone, as in *Callicebus* (see Description of New Specimens, Cranial Remains). As to the callitrichid hypothesis, Rosenberger (1977; Rosenberger et al., 1990) argued that the loss of the last molar was an independent event in callitrichines and *Xenothrix* because their dental proportions and morphology otherwise differ markedly. We agree, but on the basis of tree topology and parsimony (Horovitz and MacPhee, 1999) rather than on those differences per se.

Recently, Rosenberger (2002: 157) has altered his views somewhat and now holds that ''*Xenothrix* is a Jamaican owl monkey most closely related to *Aotus* and *Tremacebus*, which I believe are sister taxa to the *Callicebus* lineage''. From the standpoint of Rosenberger's original hypothesis concerning the relationships of *Xenothrix*, this is not a radical departure. While sister-group relationships have been rearranged, all mentioned taxa (including *Aotus*) are considered by Rosenberger to be pitheciids or pitheciid collaterals. Rosenberger's (2002: 157) assertion concerning the position of *Xenothrix* is based chiefly on his assessment of two characters, orbital enlargement and central incisor hypertrophy. These features are considered to be of great significance because ''[e]nlarged orbits and eyeballs are *the* [emphasis in original] fundamental adaptive breakthrough of owl monkeys. . . . [T]he inferred size of I^1 . . . may be linked with how a taxon exploits an adaptive zone. In the *Aotus* lineage these involve harvesting adaptations . . . ''. Guidance in making phylogenetic assessments in this case is offered in the form of a probability statement: ''we must weigh the likelihood that two regionally grouped taxa sharing unique morphological patterns with other adaptively specialized platyrrhines living elsewhere are anything but their cousins''.

Rosenberger (2002: 159) also contested our larger conclusion (Horovitz and MacPhee, 1999; MacPhee and Horovitz, 2002) that the three known Antillean monkeys (*Xenothrix*, *Paralouatta*, and *Antillothrix*) + *Callicebus* form a monophyletic group, arguing in particular that *Paralouatta* cannot be part of such a group because it is ''a howler relative, based on a comprehensive series of derived cranial features seen nowhere else but in *Alouatta*, in spite of differences in dental anatomy''. In Rosenberger's assessment, Antillean monkeys must have originated from at least two different sources within Platyrrhini (*Antillothrix* was not explicitly reviewed). Consequently, the MacPhee-Horovitz Antillean clade must be judged para- or polyphyletic, depending on how one chooses to redistribute its contents.

The only way to test phylogenetic hypotheses meaningfully is with character evidence. Since no new material of *Antillothrix* or *Paralouatta* has been reported since our latest reviews of these taxa (MacPhee et al., 1995; Horovitz and MacPhee, 1999), and since Rosenberger (2002) did not otherwise identify the ''comprehensive series of derived features'' that challenges our concept of the proper placement of *Paralouatta*, as far as these taxa are concerned there is little to test that is novel. The new craniodental material described here, however, offers precisely such an opportunity for reassessing the position of *Xenothrix*, using the tools that are most appropriate for this purpose: detailed description, character definition, and parsimony analysis (see Phylogenetic Analysis and appendices 1–3).

ABBREVIATIONS

Anatomical

a., aa.	artery (arteries)
AD	apical depth (of tooth root alveolus), measured from alveolar apex to orifice
AIOF	anterolateral section of IOF
art.	articular
BL	buccolingual(ly)
C/c	maxillary/mandibular canine (+ conventional locus number)
can.	canal
cav.	cavity
chi.	chiasma
choan.	choana, -ae
coron.	coronoid
cran.	cranial
ETH	ethmoid bone
fac.	facial
fis.	fissure
for.	foramen
fos.	fossa

FRO	frontal bone
gen.	geniohyal/genioglossal mm.
gr, grt.	great, greater
I1/i1	maxillary/mandibular incisor (+ conventional locus number)
inc.	incisor, incisive
inf.	inferior, infra
innom.	innominatum, innominate
IOF	inferior orbital fissure
LAC	lacrimal bone
lac.	lacrimal
less.	lesser
M/m	maxillary/mandibular molar (+ conventional locus number)
m., mm.	muscle, muscles
mand.	mandibular
MAX	maxillary bone
max.	maxillary
MD	mesiodistal(ly)
meas.	measurement
med.	medial
n., nn.	nerve, nerves
nas.	nasal
opt.	optic, optical
orb.	orbit, orbital
PAL	palatine bone
palat.	palatine
PAR	parietal bone
PIOF	posteromedial section of IOF
PM/pm	maxillary/mandibular premolar (+ conventional locus number)
postgl.	postglenoid
pr.	process
preinc.	preincisive
PTER	pterygoid bone
pter.	pterygoid, pterygoidal
rot.	rotundum
sin.	sinus
sph.	sphenoid, spheno-
sphenpal.	sphenopalatine
SPH	sphenoid bone
SQU	squamosal bone
surf.	surface
sut.	suture
temp.	temporal
trans.	transverse
tub.	tuberosity
v., vv.	vein, veins
VOM	vomer bone
w.	wing
ZYG	zygomatic bone
zyg.	zygomatic, zygomatico-

Institutional and Other

AMNH/CMC	American Museum of Natural History/Claremont-McKenna College joint expeditions
AMNHM	Division of Vertebrate Zoology (Mammalogy), American Museum of Natural History
BP	radiocarbon years before ''present'' (i.e., radiocarbon datum, A.D. 1950)
ch.	character
CI	consistency index
LACM	Natural History Museum of Los Angeles County
ln	natural logarithm
Ma	millions of years (ago)
MNHNCu	Museo Nacional de Historia Natural, La Habana, Cuba
MPT(s)	most parsimonious tree(s)
N	sample size
POD	proxy eyeball diameter
RC	rescaled consistency index
RI	retention index
TBR	tree bisection-reconnection
TL	tree length

LOCALITIES

New fossils attributable to the Jamaican monkey have been discovered in a number of cave sites situated along the western end of Portland Ridge, southernmost Clarendon Parish (Fincham, 1997; figs. 1, 2). Paleoecological investigations of the caves in question (Somerville, Drum, Skeleton, and Lloyd's Caves) have recently been conducted by McFarlane et al. (2002). As currently mapped (Fincham, 1997), the Jackson's Bay caves consist of some 7000 m of passageways located less than 40 m below the present surface. The so-called ''upper'' caves, which include the *Xenothrix* sites just mentioned, are dry but contain a distinctive sequence of secondary deposits (see McFarlane et al., 2002).

The environs of Portland Ridge support a low, xerophylic, sclerophyllous scrub vegetation (fig. 2A). Regional precipitation averages 1014 mm/year with a pronounced dry season of 6–10 months according to information compiled by McFarlane et al. (2002). Although this is clearly a dry environment, some populations of *Callicebus moloch* and *Aotus azarae* are able to survive today at low densities in areas that are even more arid and seasonal than southern Jamaica, but always within high forest or more diverse habitat in relation to permanent or ephemeral waterways (Stallings et al., 1989: 431). McFarlane

et al. (2002) presented various kinds of evidence to support the conclusion that conditions along this part of Jamaica's south coast were rather more mesic between 16,500 BP and 700 BP, becoming drier thereafter.

Archaeological remains are common in Jackson's Bay caves, and include human bones, cassava griddles, and petroglyphs (see Fincham, 1997). These remains are almost always superficial and are either unaffected or occasionally thinly veneered by calcite sinter. Some of the *Xenothrix* fossils were also found in completely superficial settings, but others were found buried or encrusted with matrix, suggesting that this primate enjoyed a lengthy tenure in southern Jamaica. McFarlane et al. (2002) attempted to use ^{14}C dates on gastropod shells and bat guano to establish proxy chronologies for the Jackson's Bay area during the late Quaternary. Although none of their dates is directly based on the platyrrhine fossils, it is reasonable to conclude that most or all of the bones come from contexts that are latest Pleistocene or Holocene (possibly even mid- to late Holocene). It should be noted, however, that the uncorrected age estimate of 6730 $\pm$ 110 BP, quoted by McFarlane et al. (2002) for gastropod shell from the ''*Xenothrix* level'' at Skeleton Cave, does not date either of the jaws from this site, even by association, because the cave's fill appears to have been catastrophically emplaced.

Other organic remains (including bones of birds, lizards, snakes, bats, and the endemic capromyid rodent or coney, *Geocapromys brownii*) were also sampled. These are housed in uncataloged faunal collections at the AMNH and are available for study by interested specialists.

DESCRIPTION OF NEW SPECIMENS

In this and following sections, we make continuing reference to the ''comparative set'' of taxa selected for this paper (*Aotus*, *Callicebus*, *Pithecia*, *Chiropotes*, *Cacajao*), relevant features of which are illustrated in figures 7–8 and 12–16. For the list of modern specimens utilized in this study, see appendix 3. English equivalents of anatomical names accepted by *Nomina anatomica* are preferred throughout (thus ''lesser wing of sphenoid'', not ''orbitosphenoid''), unless there is no appropriate term in human anatomy. However, numerical designations for premolar and molar loci follow the usual mammalogical conventions.[5] Finally, it should be noted that, to ensure good photographic results, the teeth of the fossil specimens were coated in order to reduce irregularities in coloration due to damage or soil pigments.

MANDIBULAR REMAINS

Rosenberger's (1977) descriptions of the type jaw and its dentition are generally excellent, and in this section we confine ourselves mostly to describing features not represented on the type.

Two left mandibular fragments (AMNHM 268001, 268004; figs. 3–6; table 1) were discovered in the course of excavations in 1995 in the Map Room, a small chamber within Skeleton Cave (fig. 1; Fincham, 1997: 333). On entry the Map Room was found to be filled with >1 m of dry silts and clays, as well as a considerable amount of breakdown and localized areas of induration. Soft sediments were taken by bucket into the main chamber for screening; excavation continued in the rear of the cave until the slope of the roof and sediment induration prevented further work. Coney and bat bones were recovered in abundance, but the monkey mandibles were the only vertebrate fossils of major paleontological significance recovered at this site. Although incomplete, AMNHM 268001 and 268004 preserve certain structures lost or damaged on the holotype and therefore add substantially to our knowledge of *Xenothrix* mandibular anatomy. Both jaws represent adult animals.

The new fossils confirm that, in the intact state, the jaw of *Xenothrix* would have resembled that of living pitheciids (and to a lesser degree, atelids and *Aotus*) in exhibiting

[5] The first and second molars of *Xenothrix* are usually homologized with the first and second molars of other platyrrhines, although in the absence of ontogenetic data on dental development in the Jamaican monkey this inference is speculative. Similarly, although we use the convention pm/PM2–4 to refer, respectively, to anterior, middle, and posterior premolars, there is no decisive evidence regarding which of the four premolar loci of the primitive primate dentition is the one that has been lost in platyrrhines.

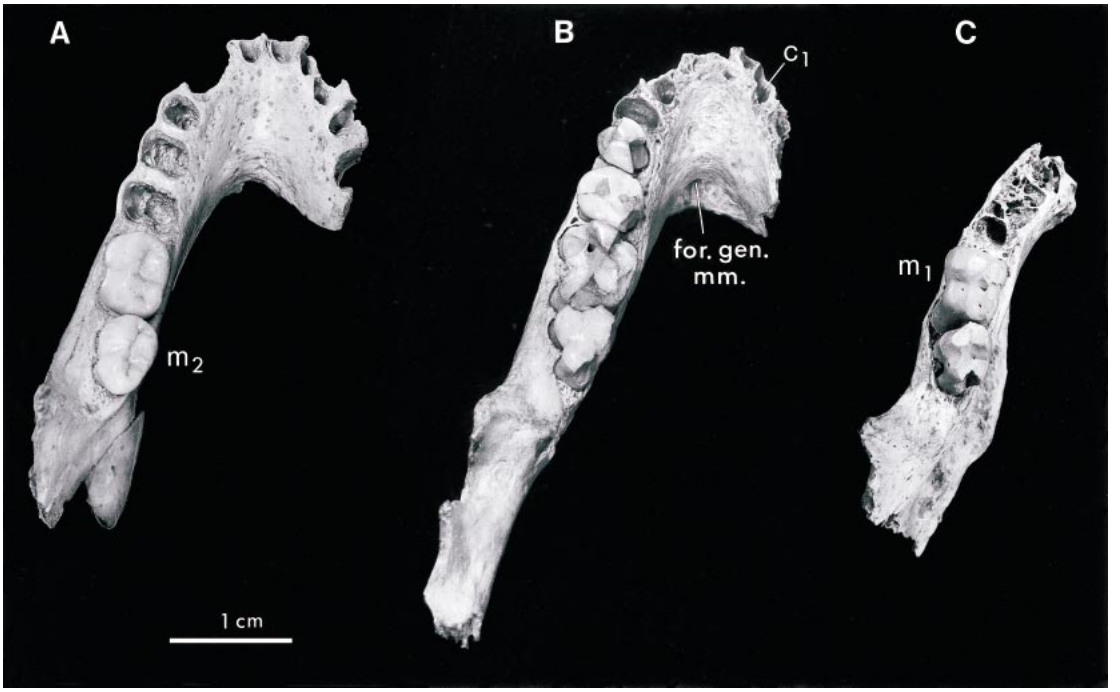

Fig. 3. Mandibular fossils of *Xenothrix mcgregori*, occlusal views and locality of recovery: (**A**) AMNHM 148198 (holotype), Long Mile Cave (Trelawny Parish); (**B**) AMNHM 268001, Skeleton Cave (Jackson's Bay, Clarendon Parish); and (**C**) AMNHM 268004, Skeleton Cave (Jackson's Bay, Clarendon Parish). Teeth in new specimens are poorly preserved due to desiccation cracking. All to scale in panel A.

a very broad ascending ramus hafted onto an anteriorly tapering corpus (''posteriorly deepening'' mandible as defined by Rosenberger, 1977; cf. figs. 7, 8). Furthermore, the large size of the individual teeth and short absolute length of the dental battery in *Xenothrix* would have given its mandible a rostrally abbreviated or foreshortened appearance, rather as in extant *Chiropotes* and *Cacajao* (fig. 8D). Average toothrow length in the two jaws that can be measured for this feature is 28.9 mm—essentially identical to extant *Pithecia* and *Chiropotes*, despite the fact that these latter taxa retain the third molar.

Reconstructions of the mandible of *Xenothrix* in occlusal and left lateral views are depicted in figure 6A and B. Because each fossil jaw possesses some anatomical details that the others lack, it is possible to reconstruct, within limits, essentially all of the corpus and ramus except for the coronoid process and the condylar and gonial areas. All likely configurations of the reconstructed horizontal rami yield a jaw with subparallel cheektooth rows. With no canines or incisors to help establish a silhouette, it is difficult to determine the likely appearance of the anterior toothrow. However, there can be no question that the individual members of the row were relatively narrow-crowned (see Discussion).

CORPUS AND RAMUS

AMNHM 268001 (figs. 3B, 4B, 5B) consists of the left ascending ramus and body as well as both sides of the symphyseal region. The entire inferior edge of the mandible has spalled off except for a small area close to the symphysis. Although the posterior border of the ramus is missing from condyle to angle, as a whole this part of the mandible is better preserved than it is in the type specimen (figs. 3A, 4A, 5A). The lateral surface of the ramus bears a shallow triangular fossa,

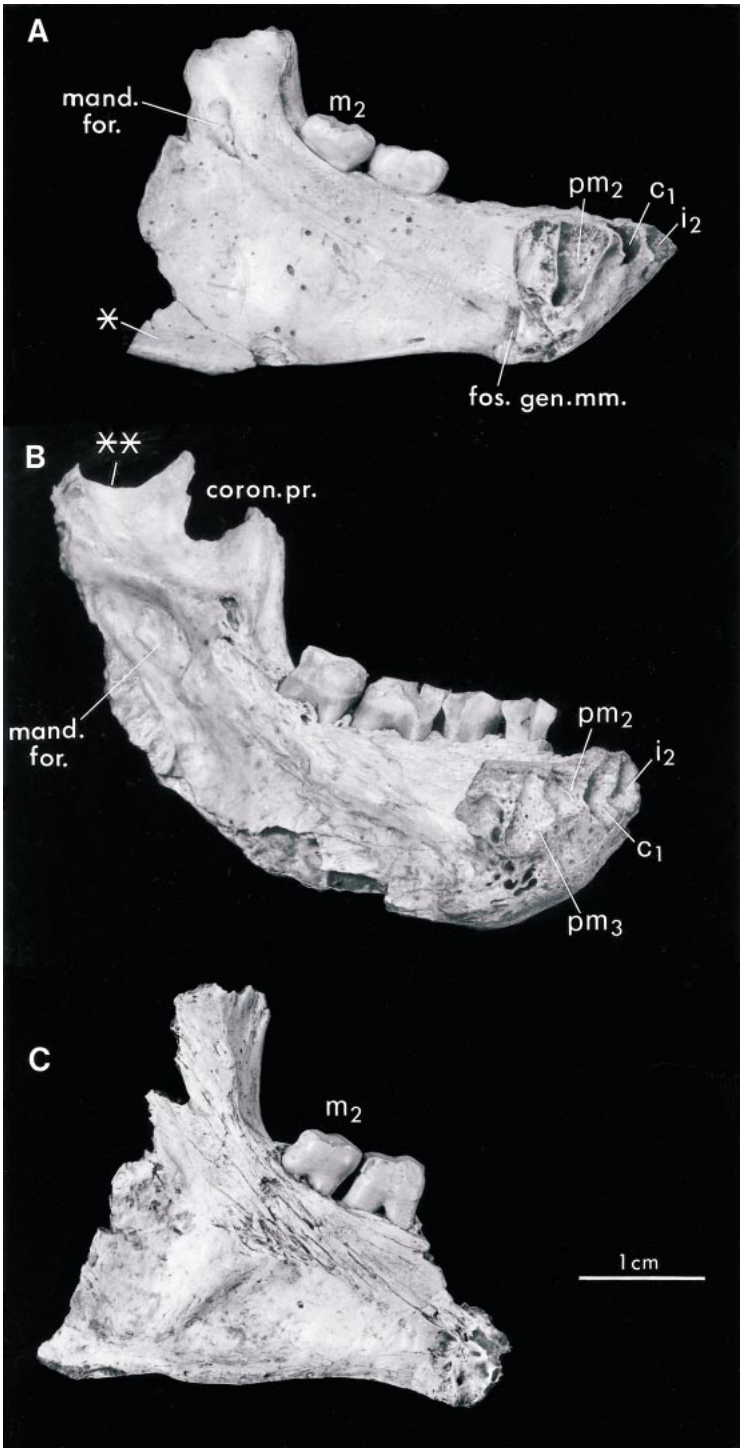

Fig. 4. Mandibular fossils of *Xenothrix mcgregori*, medial views (see fig. 3 for details): (**A**) AMNHM 148198 (holotype), (**B**) AMNHM 268001, and (**C**) AMNHM 268004. Orientation based on position of jaws as seen in pitheciid skulls placed in Frankfurt plane. *, recently attached fragment of inferior border of type mandible (see text). **, small section of mandibular notch preserved in AMNHM 268001. All to scale in panel C.

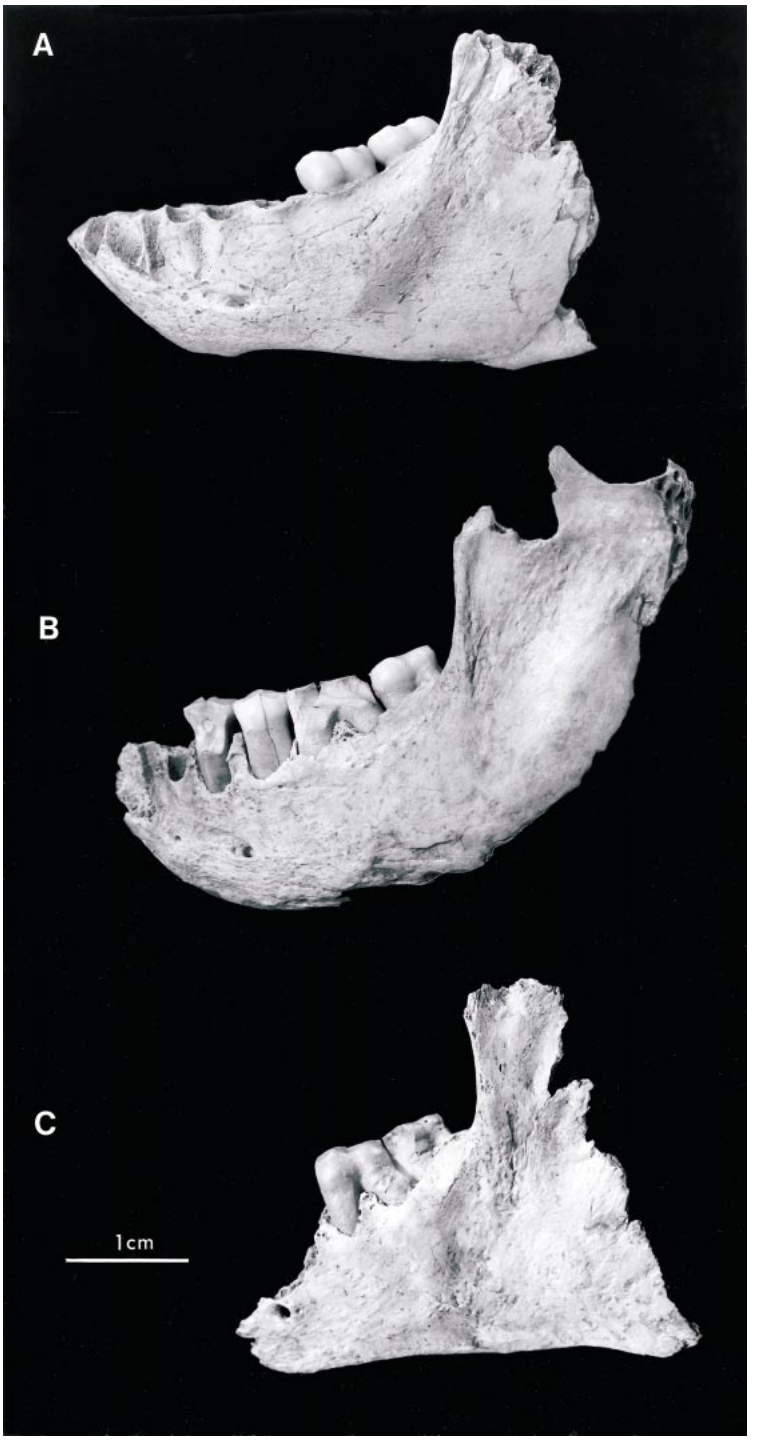

Fig. 5. Mandibular fossils of *Xenothrix mcgregori*, lateral views (see fig. 3 for details): (**A**) AMNHM 148198 (holotype), (**B**) AMNHM 268001, and (**C**) AMNHM 268004. All to scale in panel C.

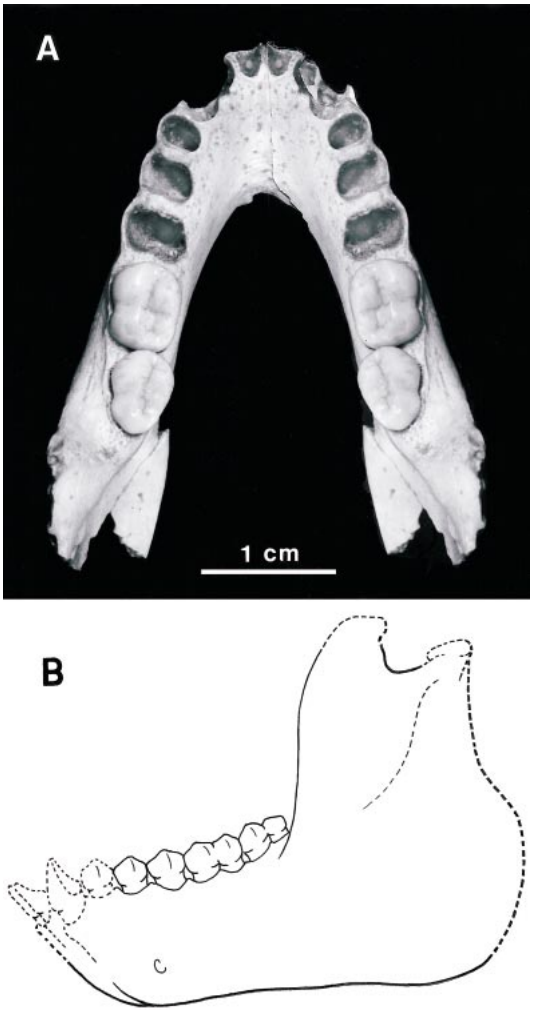

Fig. 6. Composite reconstructions of the mandible of *Xenothrix mcgregori*: (**A**) occlusal view, based on AMNHM 148198 (proper and mirror images); and (**B**) left lateral view, based on the three available jaws (AMNHM 148198, 268001, and 268004) and oriented approximately in reconstructed norma lateralis (Frankfurt plane). Dashed lines indicate features and borders still unknown. Cf. figures 7 and 8.

presumably for the insertion of part of the superficial masseter m. (area not represented on type jaw). This fossa is continued upward onto the broken root of the coronoid process, which, judging from what remains, must have been quite large. Whether the coronoid ended as a spike or was strongly recurved cannot be determined from the material available, and the reconstruction (fig. 6B) is noncommittal. On the medial side of the ramus, behind the last molar, is a large and very excavated mandibular foramen (not ''mylohyoid foramen'' of Rosenberger [1977: 470], a lapsus). Above the foramen a thick pillar of bone runs from the body of the mandible backward and slightly upward. In the intact state this pillar would have terminated as the neck of the condyle.

Remarkably, a tiny piece of cortical bone defining the inferior margin of the mandibular notch is still preserved (double asterisk, fig. 4B). This is of some interest because it gives a qualitative idea of the length of the mandibular load arm, assuming that the mandibular condyle of *Xenothrix* resembled that of other platyrrhines (i.e., in norma lateralis, superior surface of condyle situated only slightly higher than inferiormost point on mandibular notch). If this inference is correct, the effective length of the ramus (occlusal plane to condyle) in *Xenothrix* would have been rather short, as in larger-bodied pitheciids (fig. 8B–D).

As is typical for platyrrhines other than *Paralouatta*, the symphyseal region slopes sharply away beneath the incisor sockets and there is no mental eminence. By contrast, on the oral side there is a strong retromental buttress, underneath which are two deep pits for genioglossus/geniohyoid mm. As in the type, the mental foramen is located at the level of pm3. Because the canine was unquestionably small (see Dentition), the apical end of its alveolus does not swell the symphyseal planum laterally nor interrupt the smooth line of the inferior margin of the horizontal ramus, as it does in all extant noncallitrichines except *Aotus* and *Callicebus* (which likewise have small canines).

The second mandible from Skeleton Cave, AMNH 268004 (figs. 3C, 4C, 5C), consists of a small section of the corpus preserving both molars. Although the specimen as a whole is severely damaged, the inferior edge of the mandible beneath the cheekteeth is well preserved, giving a much firmer idea of the contour of this border than previously known. This specimen shows that the inferior border of the mandible in *Xenothrix* was conspicuously inflected medially, as in many other platyrrhines (including *Callicebus* and

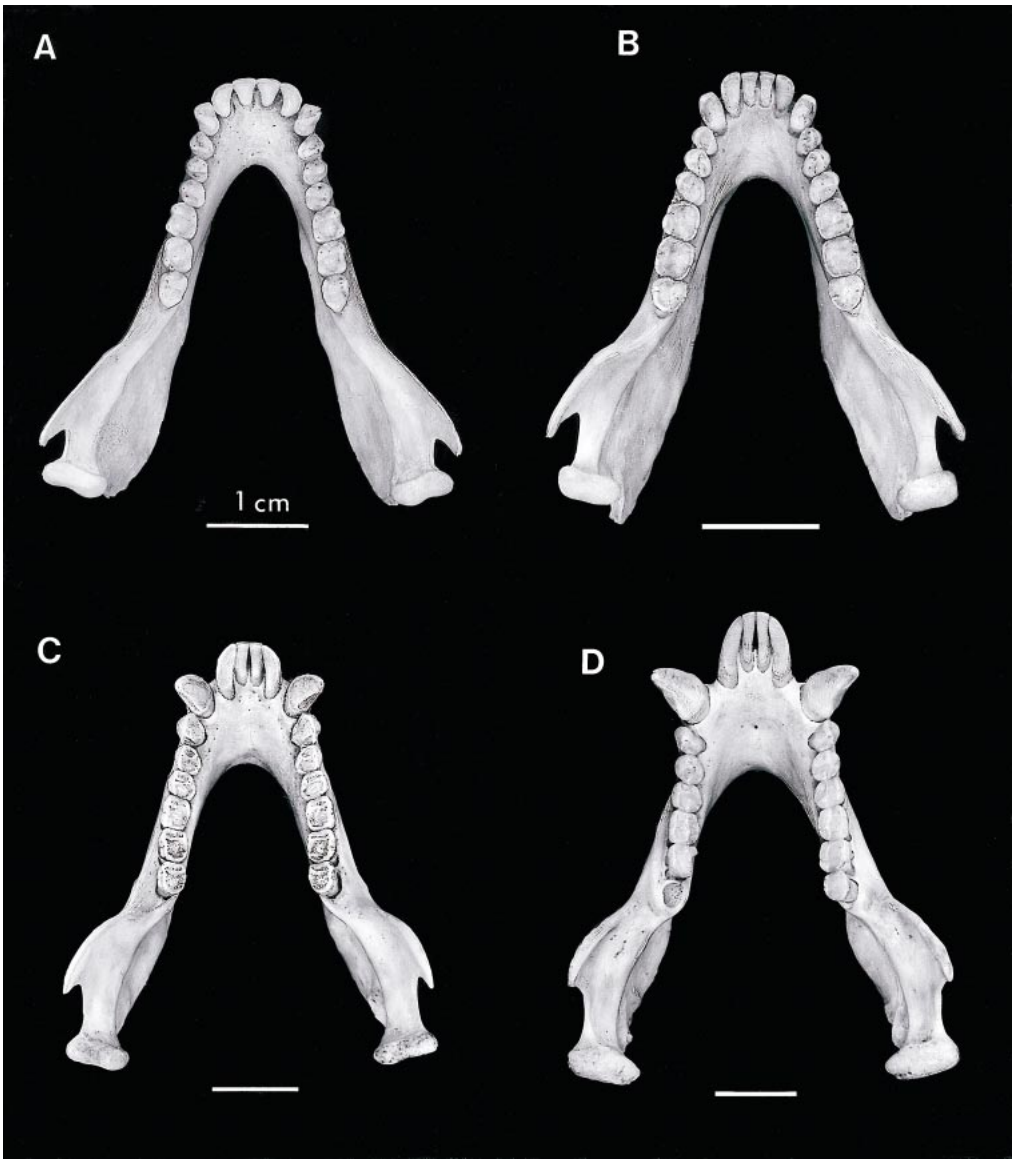

Fig. 7. Mandibles of comparative set, occlusal view: (**A**) *Aotus azarae* AMNHM 211463, (**B**) *Callicebus cupreus* AMNHM 34636, (**C**) *Pithecia pithecia* AMNHM 94133, and (**D**) *Cacajao calvus* AMNHM 73720.

Pithecia). Large ridges define the limit of an extensive, multicompartmental fossa in the gonial region for the insertion of fascicles of the medial pterygoid m. (area not represented on type jaw because of breakage).

Although it is clear that the jaw of *Xenothrix* exhibited a deep gonial region, very little of this area remains on any one specimen, making it difficult to quantify the amount of gonial flare. Rosenberger (1977: 468, fig. 3) attempted to design a mandibular profile index, but noted that because the inferior border of the *Xenothrix* type specimen was completely broken away, only ''a minimal estimate'' could be made. Thanks to the recent discovery of a small piece of the

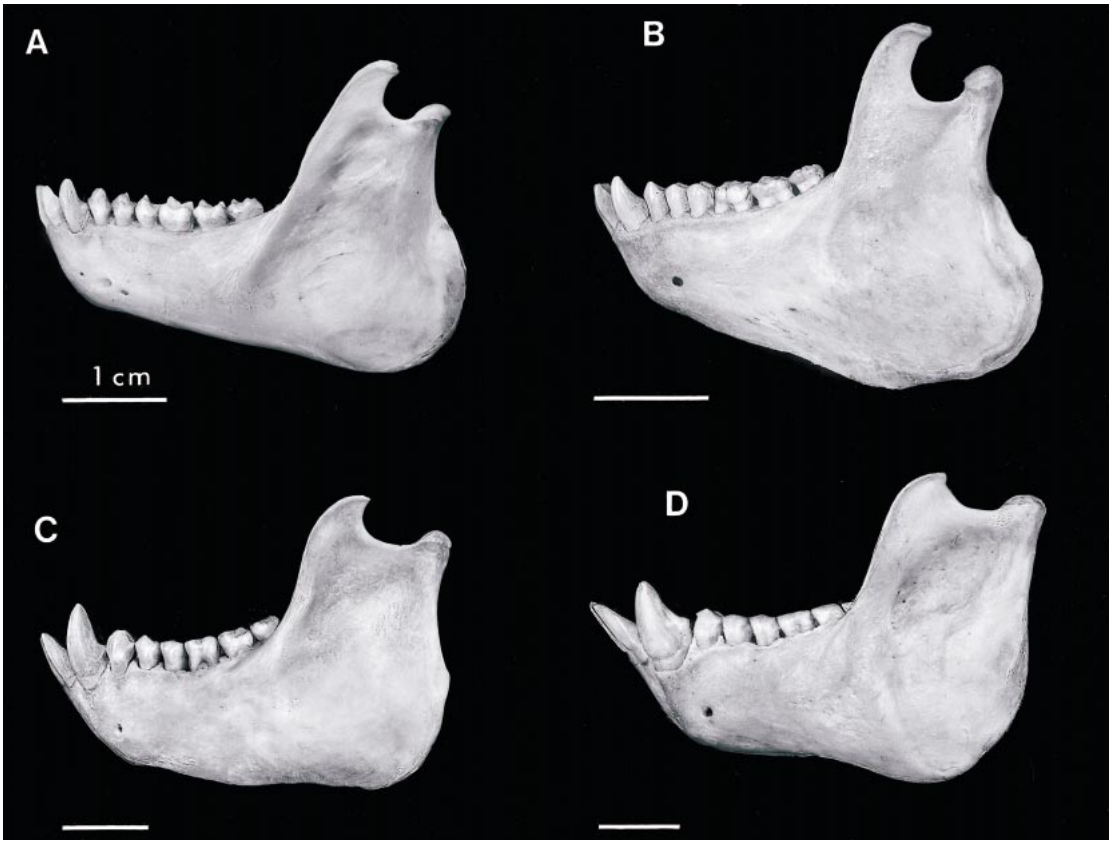

Fig. 8. Mandibles of comparative set, left lateral view: (**A**) *Aotus azarae* AMNHM 211463, (**B**) *Callicebus cupreus* AMNHM 34636, (**C**) *Pithecia pithecia* AMNHM 94133, and (**D**) *Cacajao calvus* AMNHM 73720. Specimens approximately oriented to modified Frankfurt plane.

type's inferior border (single asterisk, fig. 4A), found during recuration of H.E. Anthony's 1920 faunal collection from Long Mile Cave, it is now possible to gain a better (if still imperfect) idea of gonial flare in the Jamaican monkey. Although the area of the jaw's maximum flare is probably not represented, enough remains to allow the taking of the two measurements (symphyseal height and modified gonial height) presented in table 2. These measurements are not identical to Rosenberger's (1977), as we had difficulty in ascertaining the position of ''minimum depth'' according to his criteria. Nevertheless, except in one crucial area our results are in broad agreement. According to Rosenberger's (1977) measurements, *Xenothrix* would have expressed a degree of posterior deepening comparable to, if not more extreme than, that of *Callicebus* and *Lagothrix*. By contrast, according to our results, *Xenothrix* places closer to midsized pitheciids than to *Callicebus* for this feature. From this we conclude that *Xenothrix* possessed posterior deepening, but not in the exaggerated form seen in the titi monkey or woolly spider monkey (or, for that matter, *Aotus*). Some published photographs of the type jaw (e.g., Rosenberger, 1977: pl. 2A) make it seem as though *Xenothrix* possessed a greatly deepened gonial region, but this is due to misorientation of the specimen (symphyseal end raised excessively, thereby overemphasizing the degree of posterior deepening).

Dentition

The teeth remaining in the new mandibles are not in good condition, most having lost

TABLE 2
***Xenothrix mcgregori* and Comparative Set: Symphyseal Height and Gonial Height (in mm)**

Taxon[a]	Symphyseal height[b] (I)	Modified gonial height[c] (II)	Ratio I/II
Callicebus	7.7 (6.9–8.8)	15.9 (14.5–17.1)	0.48
Aotus	7.9 (7.7–8.0)	13.3 (11.9–14.4)	0.59
Xenothrix	12.5*	17.4	0.72
Pithecia	13.5 (12.2–15.1)	18.2 (16.4–21.0)	0.74
Chiropotes	14.8 (11.8–16.3)	18.1 (16.1–20.7)	0.82
Cacajao	16.7 (12.5–18.8)	19.7 (16.4–21.6)	0.85

[a]Taxa are listed in ascending order of value of ratio I/II. $N = 4$/taxon (except for *Xenothrix*). AMNHM accession numbers of specimens measured: *Aotus* 209916, 211458, 211460, 211463; *Callicebus* 73705, 75988, 98102, 130361; *Pithecia* 76413, 94133, 94147, 187984; *Chiropotes* 76889, 94126, 95867, 96339; *Cacajao* 73720, 76391, 98316, 98473; *Xenothrix* 268001 (for measurement I), 148198 (for measurement II). The one measurement that could not be taken accurately because of damage to specimen is followed by an asterisk (*).

[b]Vertical midsagittal distance, interproximal space between central incisors to inferior border of mandible, mean and range. For consistency in orientation of symphysis, measurement was taken as a vertical distance with inferior border resting on flat surface (table top or caliper arm).

[c]Minimum distance between inferior rim of mandibular foramen and inferior border of mandible, mean and range.

significant sections of their crowns (figs. 3–5). They are also extensively worn, both occlusally and interproximally, indicating that the new jaws came from animals that were ontogenetically somewhat older than the one represented by the holotype (the molars of which show virtually no wear). Although dental measurements for these specimens are provided in tables 3 and 4, most should be regarded as minimum estimates due to breakage and loss of material.

AMNHM 268001 preserves on the left side parts of pm3–m2 and sockets for i1–pm2 (figs. 3B, 4B, 5B). On the right side, sockets (but no teeth) are partially preserved for i1–pm1. AMNHM 268004 retains only the two left molars and the distal wall of the left pm4 socket (figs. 3C, 4C, 5C). A noticeable gap, not present in the holotype, exists between the distal margin of the m2 and the edge of the ascending ramus in both AMNHM 268001 and 268004. To confirm

TABLE 3
***Xenothrix mcgregori* and Comparative Set: Toothrow Length (TRL) (in mm)[a]**

Taxon[b]	Mandibular TRL	Maxillary TRL
Aotus ($N = 4$)	21.8 (20.9–22.9)	22.5 (21.7–23.2)
Callicebus ($N = 4$)	22.0 (20.5–22.7)	21.9 (20.1–22.9)
Pithecia ($N = 4$)	29.0 (26.8–31.0)	28.7 (26.8–31.4)
Chiropotes ($N = 4$)	30.1 (28.0–33.0)	30.5 (28.4–34.3)
Cacajao ($N = 4$)	36.6 (34.8–37.9)	36.6 (35.2–37.4)
Xenothrix AMNHM 148198	29.1	—
Xenothrix AMNHM 268001	28.7	—
Xenothrix AMNHM 268006 (L only)	—	28.2

[a]Minimum distance, labial wall of alveolus of central incisor to distal wall of same-side last molar, measured level with alveolar orifices, mean and range.

[b]AMNHM accession numbers of specimens measured: *Aotus* 209916, 211460, 211463, 239851; *Callicebus* 34636, 73705, 75988, 130361; *Pithecia* 76413, 94211, 187972, 187984; *Chiropotes* 76889, 94127, 94160, 96339; *Cacajao* 73720, 76391, 98316, 98473.

TABLE 4
***Xenothrix mcgregori*: Dental Measurements (in mm)[a]**

AMNHM No.	Locus	BL	MD
148198	m1	5.1	6.1
	m2	4.5	6.0
268001	pm3	—	3.8*
	pm4	5.2	4.1*
	m1	—	5.9*
	m2	4.9*	5.6*
268004	m1	5.2*	5.9*
	m2	4.3*	5.2*
268006	PM4	6.1	3.9
(L only)	M1	7.0*	5.1
	M2	4.5	4.1
268007	PM3	5.0	3.7
	PM4	5.7	3.8
	M1	6.6	5.2
	M2	4.8	3.7
Means	m1	5.2	6.0
	m2	4.6	5.0
	PM4	5.9	3.9
	M1	6.8	5.2
	M2	4.7	3.9

[a]Measurements that could not be taken accurately because of damage to specimen are followed by an asterisk (*).

TABLE 5
***Callicebus* and *Cacajao*: Comparative Dental Measurements (in mm)[a]**

Locus	Measurement	*Callicebus* ($N = 3$)	*Cacajao* ($N = 3$)
pm4	BL	2.8 (2.6–3.0)	4.4 (4.4–4.5)
	MD	2.6 (2.4–2.9)	3.8 (3.6–3.9)
m1	BL	3.3 (3.0–3.5)	4.3 (4.3–4.5)
	MD	3.6 (3.3–3.8)	4.4 (4.2–4.7)
m2	BL	3.3 (2.9–3.4)	4.4 (4.4–4.5)
	MD	3.7 (3.5–3.8)	4.4 (4.4–4.5)
m3	BL	2.9 (2.7–3.0)	3.7 (3.4–4.0)
	MD	3.4 (3.3–3.5)	3.9 (3.6–4.1)
PM3	BL	3.6 (3.3–3.7)	6.0 (5.9–6.2)
	MD	2.5 (2.5–2.7)	3.6 (3.5–3.6)
PM4	BL	3.3 (3.6–4.0)	5.9 (5.8–5.9)
	MD	2.5 (2.5–2.6)	3.6 (3.5–3.7)
M1	BL	4.5 (4.3-4.6)	5.2 (5.1–5.3)
	MD	3.7 (3.6–3.7)	4.4 (4.2–4.5)
M2	BL	4.2 (4.0–4.3)	4.9 (4.7–5.1)
	MD	3.5 (3.4–3.7)	4.2 (4.1–4.3)
M3	BL	2.9 (2.6–3.1)	4.3 (4.1–4.5)
	MD	2.5 (2.4–2.5)	3.5 (3.3–3.5)

[a]AMNHM accession numbers of specimens measured: *Callicebus* 73705, 75988, 130361; *Cacajao* 73720, 98316, 98473.

that this gap is not due to the presence of an unerupted m3, AMNHM 268001 was radiographed. No evidence of a crypt was found (cf. Williams and Koopman, 1952), and we conclude that the difference between jaws in this respect is probably due to intraspecific variation or is a function of age.

Despite damage to the molars, it is obvious that their occlusal surfaces were comparatively large. The few linear measurements that can be taken indicate that the occlusal area (BL × MD) of each molar is more than two times the size of individual m1s and m2s of *Callicebus* (table 5). Furthermore, summed m1–m2 occlusal area (based on mean dimensions) in *Xenothrix* is 54.2 mm^2, which is effectively identical to the average for the entire molar row in a sample ($N = 3$) of *Cacajao* (52.7 mm^2; see also table 5). This comparison is of some interest, inasmuch as *Xenothrix* was probably similar to uakaris in body size (see Discussion). This finding supports Rosenberger's (1977: 474) contention that ''in *Xenothrix* the total relative length of the molars appears to have remained stable or to have increased [compared to the primitive condition], the absolute number of components notwithstanding.''

The molars of *Xenothrix mcgregori* and *Cebus apella* are also similar in size (cf. Swindler, 2002). However, despite evident bunodonty in *Xenothrix*, its crown enamel is not relatively thickened (L. Martin, personal commun.), in contrast to *C. apella* in which extremely thick enamel apparently facilitates the mastication of palm nuts and other very hard foods. It is tempting to speculate that *Xenothrix* may have been chiefly a ''seed predator'' in the manner of the large living pitheciines (Kinzey, 1992), although we cannot offer any morphological support for this argument at present. Even within Pitheciinae, a morphologically homogeneous group, there is some dietary plasticity with regard to the intake of ripe fruits, leaves, and insects, which should make one cautious about interpreting the fossil monkey's preferences too narrowly.

The middle and posterior premolar crowns

TABLE 6
***Xenothrix mcgregori*: Measurements of Anterior Premolar and Canine Alveoli (in mm)**

Locus (alveolus)	Measurement[a]	AMNHM 268001 (L mandibular)	AMNHM 268006 (R maxillary)
pm2/PM2	AD	8.6	5.6
	BL	3.9	4.5
	MD	2.2	2.3
	VM[b]	73.8	58.0
c1/C1	AD	9.0*	9.0
	BL	4.1*	4.3
	MD	2.6*	3.5
	VM	~95.9	135.5

[a]Measurements that could not be taken accurately because of damage to specimen are followed by an asterisk (*).
[b]Volume modulus (in mm^3).

are also large and stoutly built. As Rosenberger (1977) noted, BL widths of the molars of *Xenothrix* are broad compared to those of extant platyrrhines. This also applies to the premolars: for example, the broken left pm4 of AMNHM 268001 has a BL width of ~5.2 mm, as compared to a mean of 4.4 mm for the homologous tooth in the *Cacajao* sample (tables 4, 5). The condition of the anterior premolar has to be inferred from alveolar measurements (table 6), as the tooth is not preserved in any specimen. Interestingly, the right pm2 alveolus in AMNHM 268001 seems to be unusually shallow (?anomalous retention of deciduous tooth), although so little is left of this feature that it is hard to be certain (fig. 4B). In any case, no crypt for an unerupted successor is in evidence. The left pm2 alveolus appears normal (fig. 5B). In larger pitheciines the equivalent of the curve of Spee is quite pronounced, the premolars showing a steady forward increase in crown height (fig. 7C, D). In *Callicebus* and probably also *Xenothrix* the curve is flatter, in keeping with the imputed small size of the canine (cf. figs. 6B and 7B).

Although the condition of the c1 in *Xenothrix* is not known, because there are no osteological indications of diastemata in the available jaws we agree with Rosenberger that it seems unlikely that the c1 crown could have flared either mesially or distally to any important degree. Our reconstruction (fig. 6B) suggests that c1 may have been more bulbous than the teeth on either side of it, but it probably did not project above them to any significant extent.

None of the mandibular incisors is preserved, but the close packing and parallel walls of their highly compressed alveoli suggest relatively narrow crowns (see Discussion). In the available specimens, incisor alveoli are too incomplete to determine whether the roots of the centrals were larger than those of the laterals. In Pitheciidae generally (including *Callicebus*), lateral incisor crowns are appreciably larger than those of the centrals, but roots are only slightly larger. In *Aotus*, laterals are subequal to very slightly larger than centrals for both features. Whether lower incisor crowns were relatively "heightened" (a diagnostic feature of Pitheciinae originally noted by Kinzey [1992]) cannot be decided in the absence of the teeth themselves.

CRANIAL REMAINS

Complementing the new jaws are two cranial specimens recovered in a side chamber (Xenothrix Hall) opening from Mantrap Pit, Lloyd's Cave (figs. 1, 2). Both specimens were found in cave-floor surface debris during fieldwork conducted in September 1996. Unlike the mandibular specimens, which display desiccation cracks and pigment uptake consistent with lengthy burial, the cranial specimens appear similar in apparent freshness to the numerous remains of goats and other domestic animals which litter the floor of this and other Portland Ridge caves. Lack of staining is consistent with the possibility that the skull remains from this site are not particularly old.

AMNHM 268006 is a partial face preserving the lower parts of the orbits and nasal complex, together with the entire palate and PM4–M2 on both sides (figs. 9, 10). AMNHM 268007 consists of a left maxillary fragment only, retaining PM3–M2 still in position and the alveolus of PM2 (fig. 11). Direct comparison of these specimens with skulls of other platyrrhines indicates that, contra Rosenberger (1977: 475), skull size in *Xenothrix* is significantly larger than in *Aotus* or *Callicebus* (see below).

Not unexpectedly, the new material con-

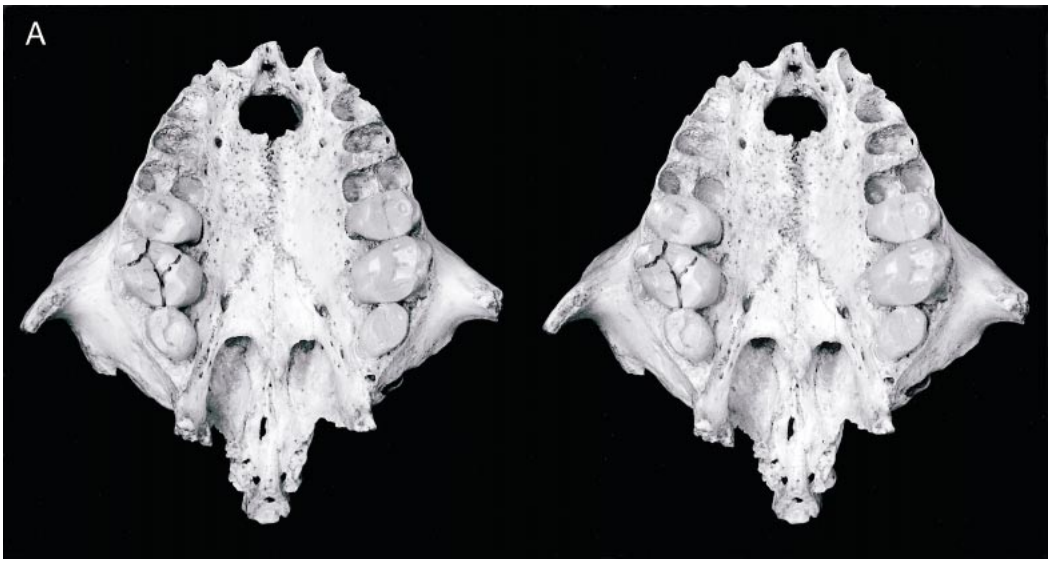

Fig. 9A. *Xenothrix mcgregori* AMNHM 268006, partial face and palate (Lloyd's Cave, Clarendon Parish). Stereopair views (with keys) on this and following pages: (**A**) ventral (occlusal), (**B**) dorsal, (**C**) rostral, (**D**) caudal, and (**E**) right lateral. *, aperture in presphenoid (?natural); **, anterior portion of zygomaticomaxillary suture; ***, groove marking the anterior end of the infraorbital fissure; ****, eminence marking the medial border of the optic canal. All to scale in panel A.

firms that only two molar loci occur in the maxillary dentition of *Xenothrix mcgregori*, whose dental formula (2/2 1/1 3/3 2/2) is unique within noncallitrichine Anthropoidea.

Facial Skeleton and Orbits

As preserved, AMNHM 268006 is reasonably intact (figs. 9, 10; table 6): the alveolar process of the maxilla and palate are com-

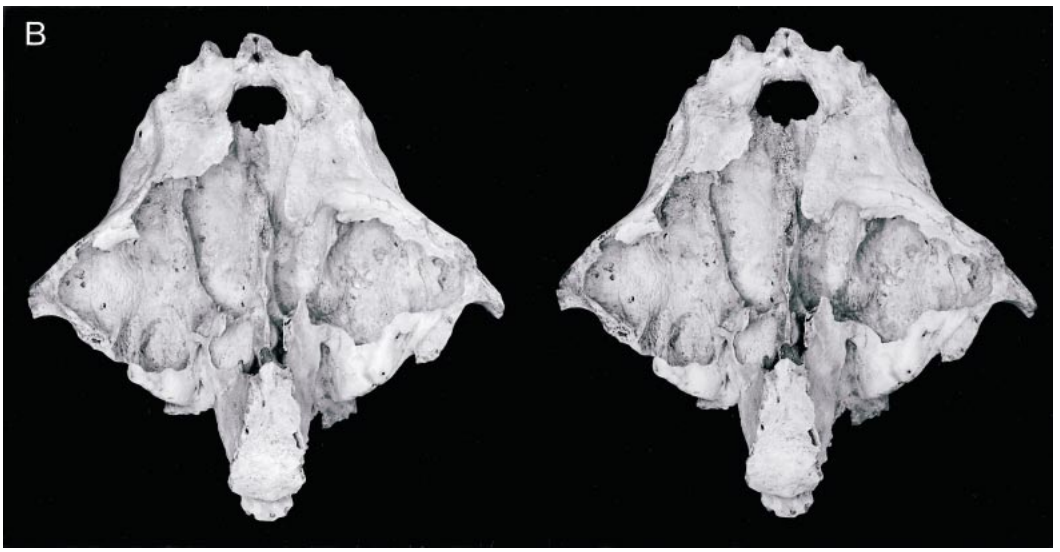

Fig. 9B.

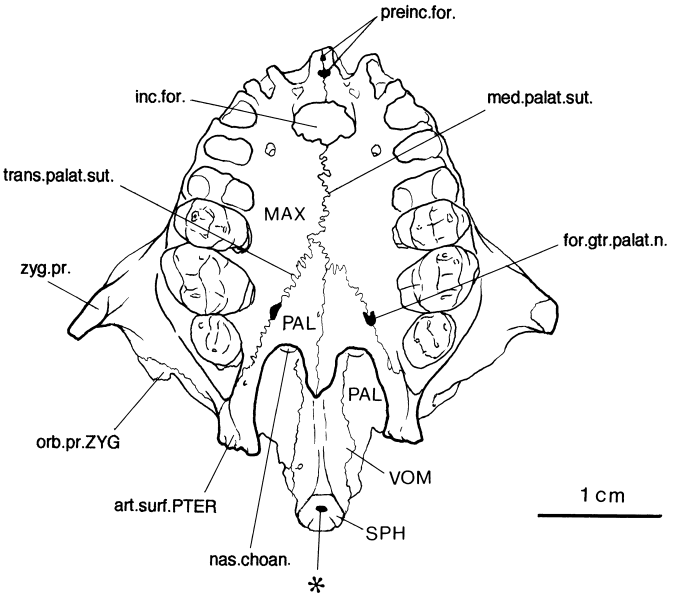

Fig. 9A Continued.

plete except for minor abrasions, and substantial portions of the sphenoid, palatines, vomer, lacrimal, and interorbital septum remain. Other parts of the face, including the upper orbits and most of the orbital floors, zygomatics, and upper nasal cavity were evidently broken away some time ago, as no fresh breaks can be seen in the relevant areas.

Morphological evaluations of the midfacial, nasal, and palatal regions are provided in subsequent sections of this paper. It is unfortunate that so little is left of the orbital

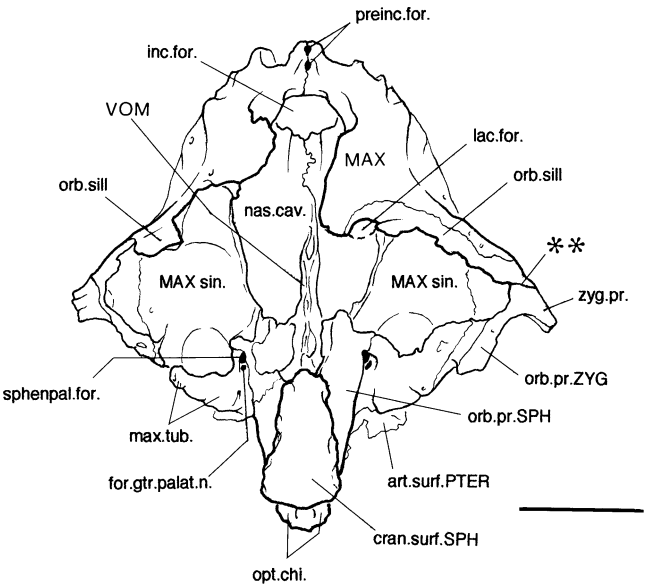

Fig. 9B Continued.

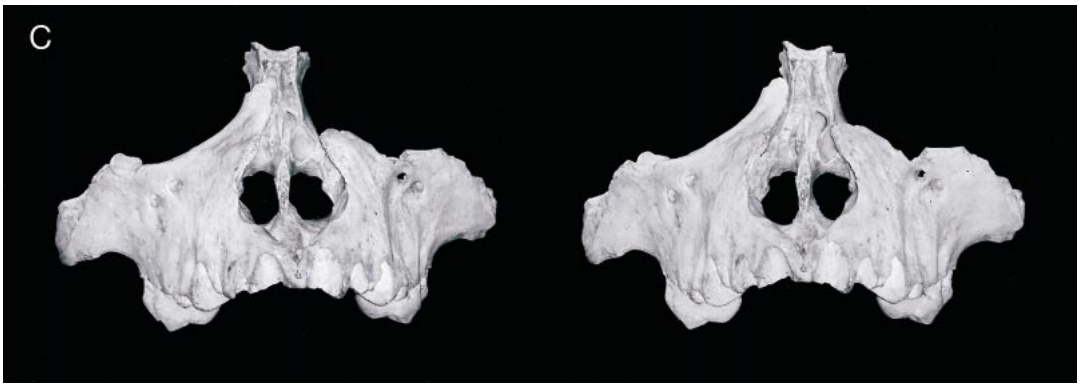

Fig. 9C.

skeleton in AMNHM 268006, since the plausibility of Rosenberger's *Aotus* hypothesis largely turns on his interpretation of its morphology. Features connected with the eye and orbit of *Xenothrix* are reserved for separate treatment (see Discussion).

MIDFACIAL REGION: The midfacial region is a relatively smooth, undulating surface between the inferior rims of the orbits and maxillary alveolar process (fig. 9C). The infranasal planum—the zone on the premaxillae below the nasal sill—varies greatly in morphology among platyrrhines, especially in regard to prognathism. This can best be appreciated by viewing skulls in norma dorsalis (in modified Frankfurt plane, as defined in appendix 1, ch. 85). Seen from above, midfacial prognathism in *Aotus* (fig. 12E) is notably less than that of any other member of the comparative set (fig. 12F–H). *Callicebus* (fig. 12F) is less prognathic than the other extant pitheciids, which may display exceptional protrusion of the premaxillae and incisor row (Hershkovitz, 1977; Rosenberger, 1992). The partial face of *Xenothrix* (fig. 9B, E) can only be roughly aligned along the Frankfurt plane, but its degree of midfacial prominence is clearly greater than that of *Aotus*.

The canine fossa, a feature found in most noncallitrichines and all pitheciids except *Callicebus* (in which it is indistinct), is absent or barely indicated in *Xenothrix*. The indistinct/absent condition is obviously correlated with the small size of the canine root (see Dentition). Double infraorbital foramina occur bilaterally in AMNHM 268006 (fig. 9C); the more posterior of the two is larger and situated vertically above the PM3 alveolus. Multiple infraorbital foramina are found in many species of New World monkeys, and foraminal number can vary be-

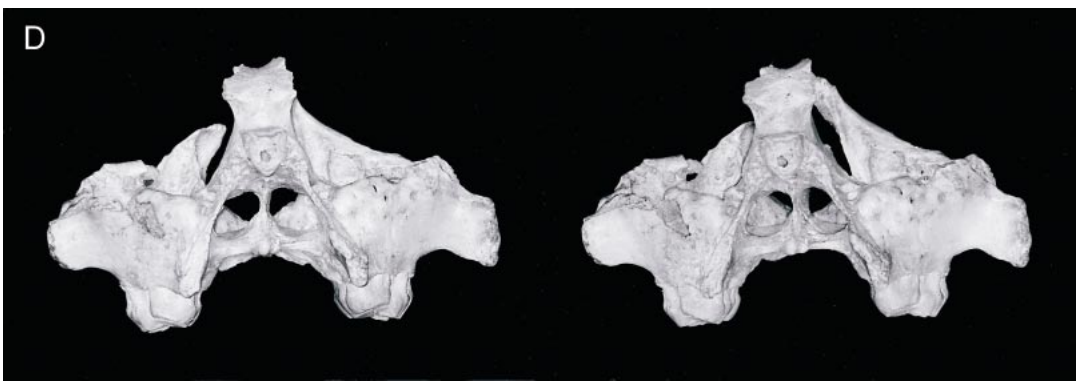

Fig. 9D.

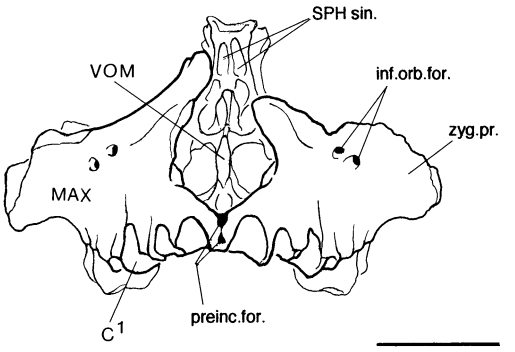

Fig. 9C Continued.

tween and even within individuals (Hershkovitz, 1977).

New World monkeys display differences in the vertical positioning of the maxillary root of the zygomatic arch. In some, including living pitheciids and atelids, the zygomatic arches have a high root, whereas in others (e.g., *Callicebus*, *Cebupithecia*, *Paralouatta*, *Aotus*) the root is much lower. Among living platyrrhines, *Aotus* (fig. 14A) and *Callicebus* (fig. 14B) show an extreme condition in which the lowest part of the zygomatic arch extends below the horizontal level of the alveolar process in norma lateralis. In *Callicebus* the arch actually extends to a level below the occlusal plane of M3 (fig. 14B). In *Xenothrix* a less extreme condition is seen, in which the lowest point on the arch extends slightly below the level of the M2 alveolar margin. In the photographs this feature is best seen in figure 9E. (This feature is not complete enough in *Paralouatta* to permit evaluation, and the maxillary fragment of *Antillothrix* does not retain the arch; cf. MacPhee and Horovitz [2002].) A complication in scoring this character is that in some large males of *Pithecia* and *Cacajao* the origin of masseter m. (which springs from the lowest point on the zygomatic arch) is hypertrophied into a downwardly projecting crest, thus mimicking to some degree the condition in platyrrhines with depressed arches (fig. 13D). However, with careful inspection these conditions can be distinguished.

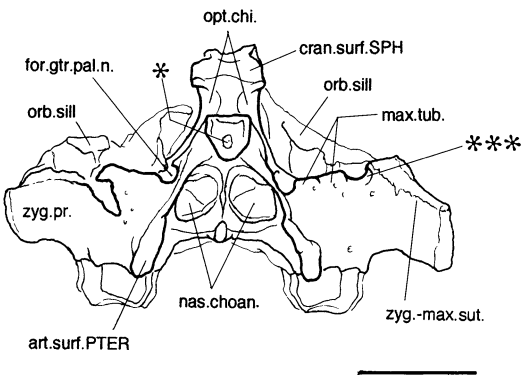

Fig. 9D Continued.

In AMNHM 268006 the relatively dorsal position of the suture between the zygomatic bone and the anterior part of the maxillary root of the zygomatic arch indicates that the former's contribution to the lateral orbital wall was less extensive than in some extant pitheciids, but much more so than in *Aotus*. It is critical to note that a small portion of the orbital wing of the zygomatic bone is preserved on the right side of this specimen (fig. 9B, E). Equally important is the small notch that defines the posterior edge of this process (triple asterisk, fig. 9D), as it represents the anterior limit of the inferior orbital fissure (IOF). The conformation of this area indicates that this part of the fissure could not have been widely dehiscent, as it is in *Aotus*, but instead resembled that of most New World monkeys. We reserve further remarks on these matters until the Discussion, as they bear on orbital size in *Xenothrix* and alleged resemblances to conditions in *Aotus*.

A small groove on the upper, broken side of the maxillary root near the track of the zygomaticofacial suture (double asterisk, fig. 9B) may mark the track of the zygomaticofacial nerve and accompanying vasculature. The zygomaticofacial foramen, which penetrates the body of the orbital surface of the zygomatic, is sometimes large in platyrrhines (e.g., *Callicebus*) and is often multiple. Zygomaticotemporal foramina (regarded here as equivalent to ''lateral orbital fissure'' of Hershkovitz, 1977) typically occur high on the lateral orbital wall and are not preserved in the *Xenothrix* material.

NASAL CAVITY AND PARANASAL SINUSES: In *Xenothrix* the nasal aperture was apparently wide in comparison to the breadth of the face, as in pitheciids generally. Because the nasals and most of the nasal processes of the

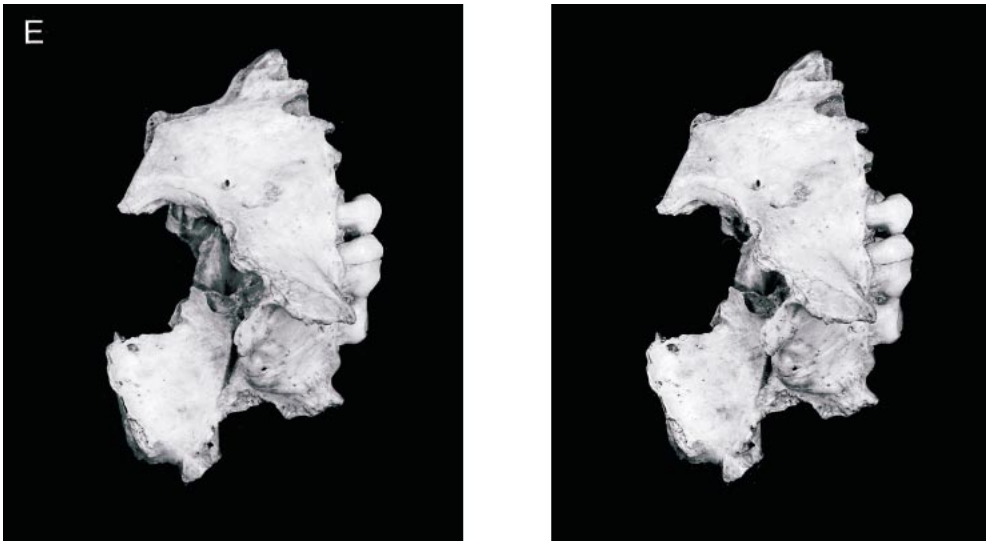

Fig. 9E.

maxillae are missing (fig. 9B, C), it is not possible to reconstruct in detail the shape of this opening when the skull was intact. However, indications are that it was probably diamond shaped with a notched upper margin (as in most extant pitheciines) rather than triangular with a broad, straight upper margin (as in *Pithecia* specifically).

The skull of *Xenothrix* was evidently highly pneumatized, although existing fossils are not well enough preserved to give a complete picture of the degree of inflation in the upper face and central stem. Thanks to fortuitous breaks in AMNHM 268006, it can be seen that air spaces deeply invade the base of the zygomatic arch and the body of the maxillae, thereby inflating much of the lateral part of the lower face (figs. 9B, 10). Even the anatomical nasal cavity is relatively widened: *Xenothrix* and also *Paralouatta* seem to be unique among known platyrrhines (including *Alouatta*) in having nasal cavity floors that are posteriorly wider than the distance between the lingual walls of the left and right M1s. More anteriorly, the rim of the inferior meatus intersects a parasagittal plane that lies

Fig. 10. *Xenothrix mcgregori* AMNHM 268006, partial face and palate (Lloyd's Cave, Clarendon Parish). Stereopair, oblique left lateral view, to show pneumatization of nasal floor and zygomatic process of maxilla. *, grooves for optic nerve (position of optic chiasma). Same scale as figure 9.

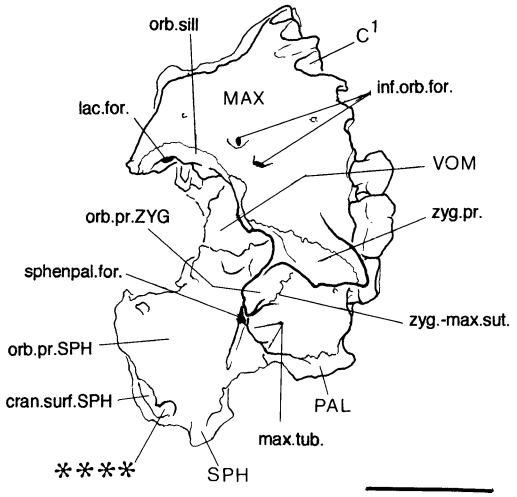

Fig. 9E Continued.

external (buccal) to the canine alveolus, another evocation of the same unique feature.

The maxillary paranasal sinuses seem to have been single, very large spaces with little or no subdivision. Mental reconstruction of their volume suggests that together they would have enclosed a space larger than the anatomical nasal cavity per se. Cheektooth roots can be seen emerging within the lateral parts of the sinuses in both cranial fossils (figs. 9B, 11A) as far as the coronal plane of PM3. In AMNHM 268007, the bone tissue draping cheektooth roots is even more excavated than in AMNHM 268006, suggesting that in the former individual sinus development was very marked.

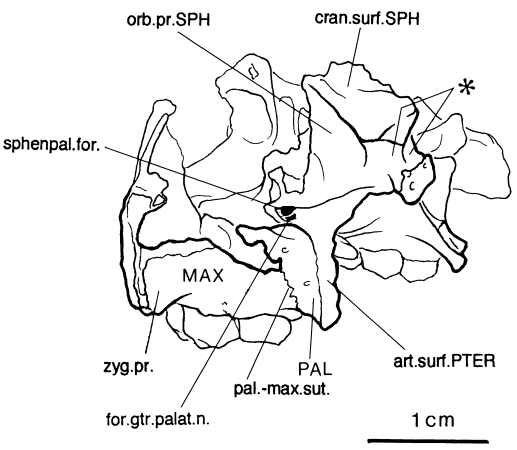

Fig. 10. Continued.

The maxillary tuberosity of the maxilla, the area posterior and superior to the last molar locus, is at least marginally inflated by the maxillary sinus in all platyrrhines (Hershkovitz, 1977). In *Xenothrix*, the degree of inflation is notable, in keeping with the pneumatization of the rest of the paranasal complex (figs. 9B, 10). Pitheciids as a group (including *Callicebus*) display well pneumatized maxillary tuberosities (fig. 16B–D). In *Aotus* (fig. 16A), by contrast, this area is flattened and the interior is spongiform or only slightly pneumatized by very small cellules (as opposed to the large chambers in pitheciids and *Xenothrix* as well as many other platyrrhines). It is worth remarking in this context that the maxillary sinus of the Miocene Patagonian species *Tremacebus harringtoni* has been described as being both ''poorly developed'' and ''as in *Aotus*'' by Fleagle and Rosenberger (1983: 144) as well as ''probably . . . large, more like *Xenothrix* perhaps'' by Rosenberger (2002: 157). In view of the comparative size of the maxillary excavations in *Aotus* and *Xenothrix*, as detailed here, these statements must be regarded as mutually contradictory.

PALATE AND ADJACENT REGIONS: The maxillary dental arcade of *Xenothrix* may be described as roughly U-shaped (fig. 9A), as in *Aotus* (fig. 12A), *Callicebus* (fig. 12B), *Saimiri*, and most other noncallitrichine platyrrhines. The maxillae are in contact along the palatal midline up to the level of the last premolar, at which point the palatine bones are interposed. A large greater palatine foramen perforates each leg of the palatomaxillary suture, which is shaped like an inverted V. The palatal surfaces of the premaxillomaxillary sutures have been completely resorbed, although externally a remnant of the midline suture between the right and left premaxillae (premaxillopremaxillary suture) is still in evidence (fig. 9B). Palatal length (prosthion–staphylion) is 28.4 mm, compared to 19.5 mm in *Callicebus* ($N = 3$) and 31.0 mm in *Cacajao* ($N = 3$).

The incisive fossa and incisive foramina together form one large, undivided hole due to the loss of the delicate spines that generally subdivide these apertures in platyrrhines (fig. 9B). Nevertheless, the large size of both the nasal cavity and the incisive ''foramen''

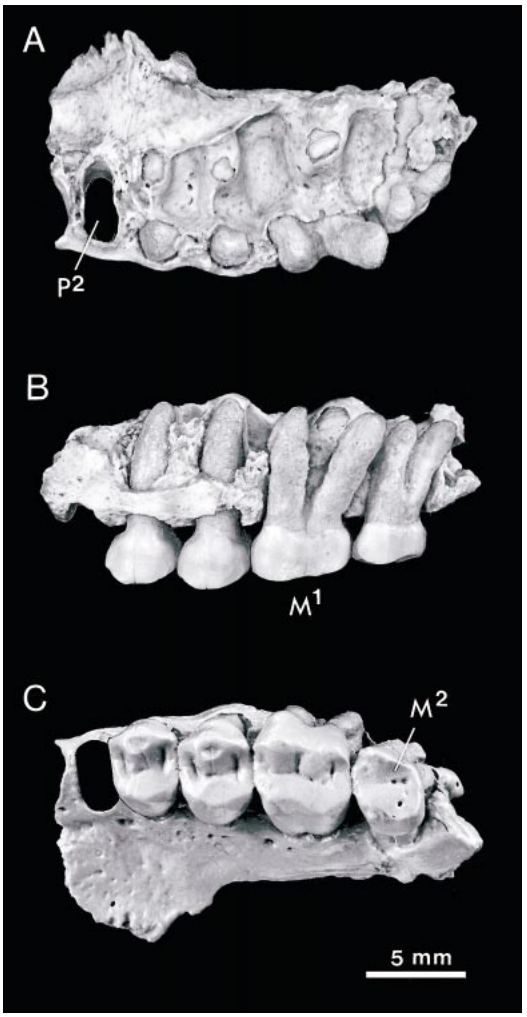

Fig. 11. *Xenothrix mcgregori* AMNHM 268007, cast of partial left maxilla (Lloyd's Cave, Clarendon Parish): (**A**) dorsal, (**B**) lateral, and (**C**) ventral (occlusal) views. All to scale in panel A.

in *Xenothrix* may be structurally and functionally linked. In living mammals, the incisive foramina give passage to the nasopalatine duct and its associated cartilage. The duct connects the oral cavity with the vomeronasal organ (Jacobson's organ), which contains specialized sensory cells related to the first cranial (olfactory) nerve. Since the cartilages of the nasal floor are highly developed in all platyrrhine taxa and the vomeronasal organ is universally present (Maier, 1980), hypertrophy of these features in *Xenothrix* is a distinct possibility.

Two rather large preincisive foramina penetrate the remnant premaxillopremaxillary suture (fig. 9A–C). They may have carried an anastomotic link between the superior labial a. (of the facial a.) and the greater palatine a. (of the maxillary a.). Foramina in this position seem to be common in platyrrhines, although to our knowledge their homologies have not been addressed.

Because of breakage, the central part of the sphenoid complex of AMNHM 268006 has been reduced to a narrow cube consisting of the body of the presphenoid and portions of the orbital surfaces (plates) of the sphenoidal greater wings (fig. 9B, E). The orbital plates are separated by two large sphenoidal sinuses (fig. 9C), divided by a septum that would have originally connected with the superior meatus of the nasal cavity. The septum is in turn continuous inferiorly with the blade of the vomer. It is doubtful that any part of the ethmoid is still present on this specimen. Although the optic canal is not preserved as such on either side, its position can be readily located by reference to the sella turcica, optic chiasma, and a small eminence on the sphenoidal orbital plate that acted as the canal's medial wall (fig. 9E). Reconstructing the position of the optic canal is helpful in trying to estimate orbital depth (see fig. 15 and Discussion).

Caudally, a large aperture opens onto the presphenoid's synchondral surface (at the presphenoid–basisphenoid synchondrosis) and communicates with the sphenoidal sinuses (fig. 9A, D). There are several other holes in the body of the presphenoid of AMNHM 268006, but these are definitely artifacts. If the aperture in the synchondral surface is real, its existence indicates that paranasal pneumatization extended into the corpus of the basisphenoid.

Two canals can be detected in the triangular slot that represents one wall of the original pterygopalatine fossa (figs. 9D, 10). The larger, the sphenopalatine foramen, passes anteriorly through the lateral wall of the nasal cavity. It would have accommodated the sphenopalatine a. and the superior nasal and nasopalatine nn. The other canal passes inferiorly through the sidewalls of the choanae,

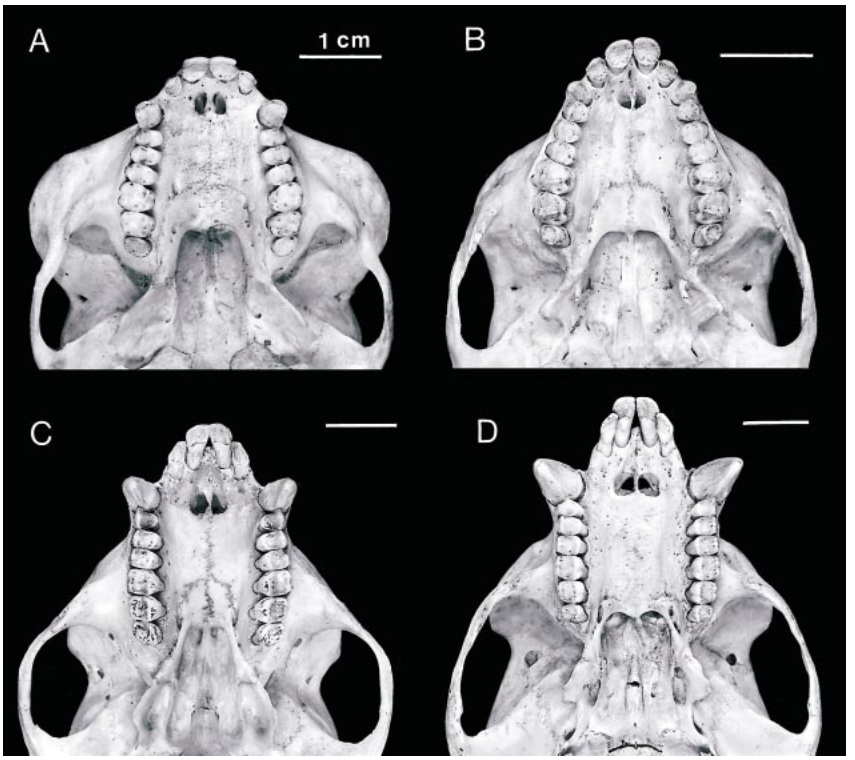

Fig. 12. Skulls of comparative set in modified Frankfurt plane (see text), ventral and dorsal views: (**A, E**) *Aotus azarae* AMNHM 211463, (**B, F**) *Callicebus cupreus* AMNHM 34636, (**C, G**) *Pithecia pithecia* AMNHM 94133, and (**D, H**) *Cacajao calvus* AMNHM 73720. In norma ventralis, interpterygoid region to level of basisphenoid–basioccipital synchondrosis also illustrated. Apparent degree of prognathism as seen in norma dorsalis should be compared to conditions in norma lateralis (fig. 14).

to terminate as noted above as the greater palatine foramen on the palate. As in *Homo*, the canals run in part along the sutural contact between the sphenoid and palatine bones.

Part of the lacrimal area is preserved on the right side of the skull, in relation to the orbital rim of the nasal process of the maxilla (fig. 9C). Because neither the posterior lacrimal crest nor the related portion of the ethmoid is preserved, the lumen of the osseous canal of the nasolacrimal duct is exposed (fig. 9B). In life the lacrimal groove, which is only partly preserved, would have been entirely encased within the lacrimal bone.

The vomer is well preserved except along its anterior edge where it made contact with the nasal septal cartilage (fig. 9C, E). In the comparative set, each ala vomeris extends posteriorly as a thin sheath along the sides of the presphenoid, variably restricting or preventing contact between the posterior parts of the palatine and the body of the presphenoid. *Cebus* and *Alouatta* are distinctive in that the alae reach the position of the pterygoid and thereby completely exclude ventral palatopresphenoid contact. Conditions in *Xenothrix* are ambiguous because of breakage.

The pterygoid bones are not preserved, but each palatine bone terminates posteriorly in a distinct spine and sutural surface which would have braced the pterygoid plates during life (fig. 9D).

DENTITION

As in the case of the mandibles, the cranial fossils preserve only molars and some premolars (figs. 9, 11). However, unlike the teeth in the jaws, the maxillary cheektooth crowns are beautifully preserved except in

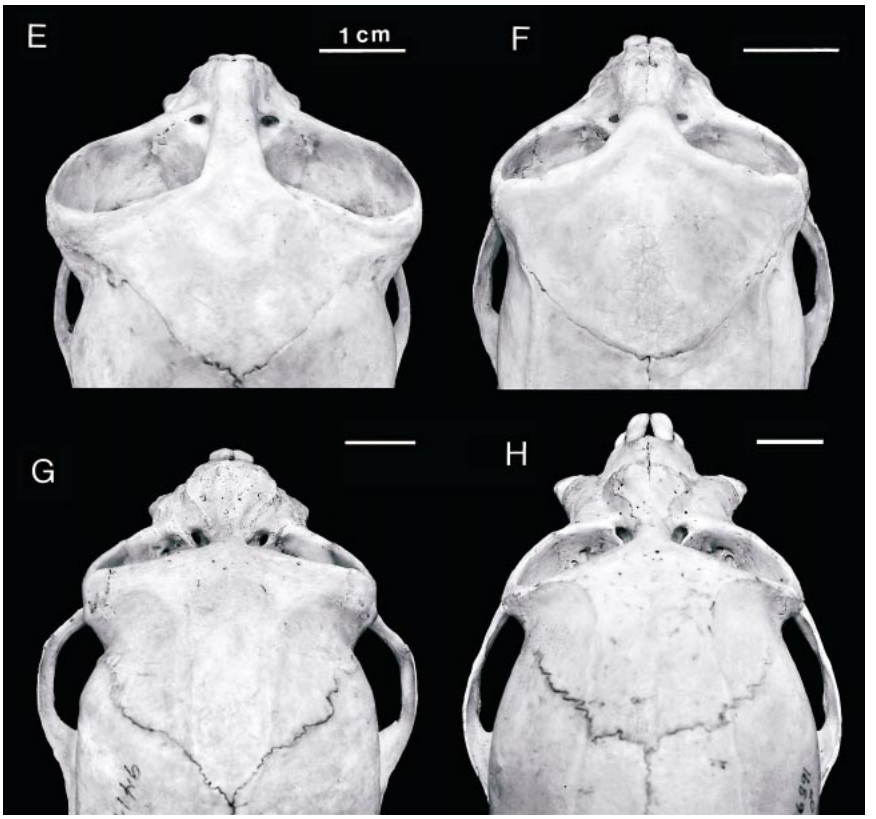

Fig. 12. Continued.

one instance (right M1 of AMNHM 268006). Alveoli of missing teeth are also largely intact in AMNHM 268006, providing some idea of the relative sizes of the roots of the anterior teeth.

Like the mandibular cheekteeth, the maxillary molars and premolars of *Xenothrix* are large and ovoid to quadrangular in outline. Principal cusps are swollen, with puffed-out shoulders that obscure the presence of cristae. Buccal cingula are absent, and lingual cingula are inconspicuous or absent. In size and to some degree in shape the upper cheekteeth of *Xenothrix* strongly resemble those of larger pitheciines (*Chiropotes* and *Cacajao*) rather than *Callicebus*. Indeed, in most metrical regards the cheekteeth of *Xenothrix* can be described as superficially uakarilike (tables 4, 5), although of course there are differences in detail. In comparison to *Cacajao* (fig. 12D) the following features of *Xenothrix* are noteworthy: (1) Principal cusps and general crown outlines are puffier in *Xenothrix*. (2) M1 of *Xenothrix* is very large and expresses unusual development of buccal moiety. (3) M2 is quite reduced, like M3 in living pitheciids (Kinzey, 1992). (4) Premolars are very large and similar in BL and MD dimensions to those of *Cacajao* (tables 4, 5). (5) PM4 is premolariform as in *Callicebus*, not distinctly molariform as in pitheciines. (6) Roots of cheekteeth are strongly divaricating, as in *Cacajao* and to a lesser degree in other pitheciids. (7) Arrangement of principal cusps and other small-scale features is very similar, except that whereas the cheekteeth of *Chiropotes* and *Cacajao* wear into what may be described as an aligned series of troughs, the main cusps and principal blades of *Xenothrix* tend to retain more definition, as in *Callicebus* (fig. 12B) or *Pithecia* (fig. 12C). (8) *Xenothrix* is distinctively

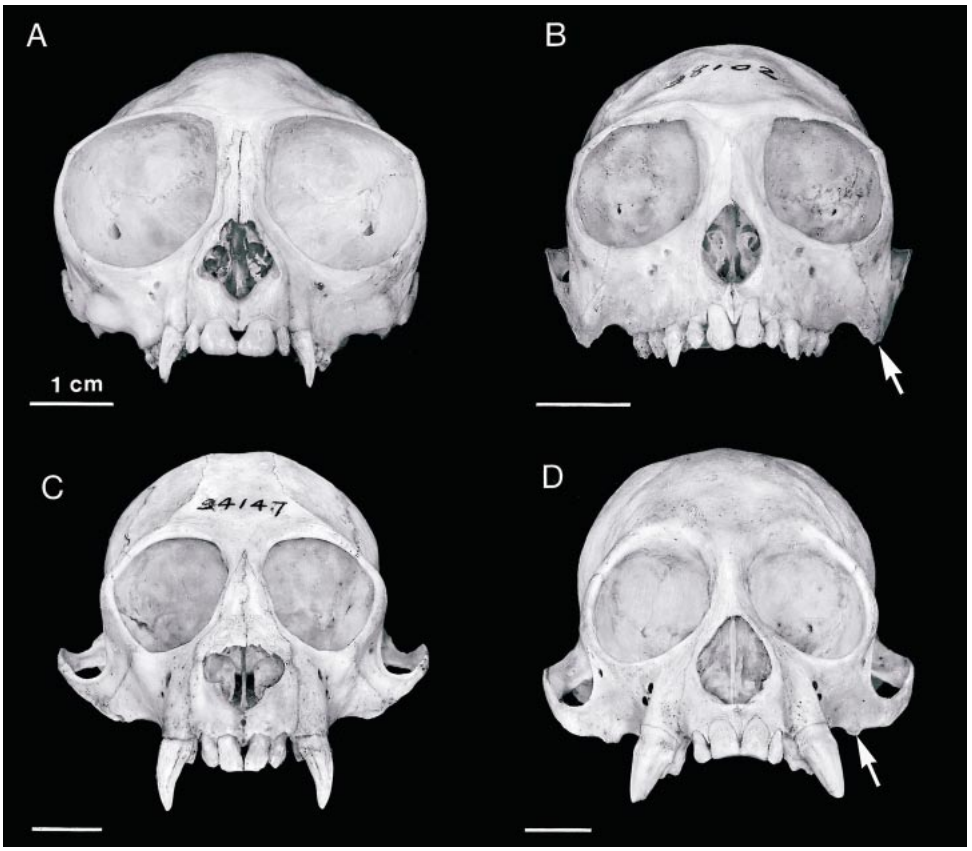

Fig. 13. Skulls of comparative set in modified Frankfurt plane (see text), anterior view: (**A**) *Aotus azarae* AMNHM 211463, (**B**) *Callicebus cupreus* AMNHM 34636, (**C**) *Pithecia pithecia* AMNHM 94133, and (**D**) *Cacajao calvus* AMNHM 73720. Arrows in B and D identify inferior margin of zygomatic process. In *Callicebus* (B) the inferior margin extends below alveolar border of molars. Other extant pitheciids do not show this character, although in some individuals the origin of masseter m. is sometimes built out into a separate dependent process, as in the specimen of *Cacajao* (D) illustrated here.

different in lacking the intense pitting, crenulation, and slight polycuspidation which uniquely distinguish cheektooth occlusal surfaces of living pitheciines. In *Callicebus* crenulation is much weaker than in pitheciines. Regarding this last feature, Rosenberger (1977) came to a different conclusion, arguing that there was some evidence of ''enamel papillation'' on lower molars of *Xenothrix*. Slight crevices and ripples can be detected under magnification, but they are no more frequent or obvious than in many nonpitheciids. Similar remarks apply to the upper molars of *Xenothrix*.

There are four cusps present on the M1 of *Xenothrix*; in our examples, the protocone and hypocone are less well defined than the paracone and metacone. The trigon and talon are indistinctly separated by a vaguely defined postprotocrista running from metacone to protocone. The hypocone is worn flat in both specimens and is associated buccodistally with a small fossette (fig. 11C). The result of this configuration is a large distal shelf or wear surface, as seen in pitheciids generally (especially in larger species, cf. fig. 12C, D). The paracone bulges outward (buccally) to a greater extent than does the metacone (figs. 9A, 11C), with the result that the tooth is markedly wider proximally than dis-

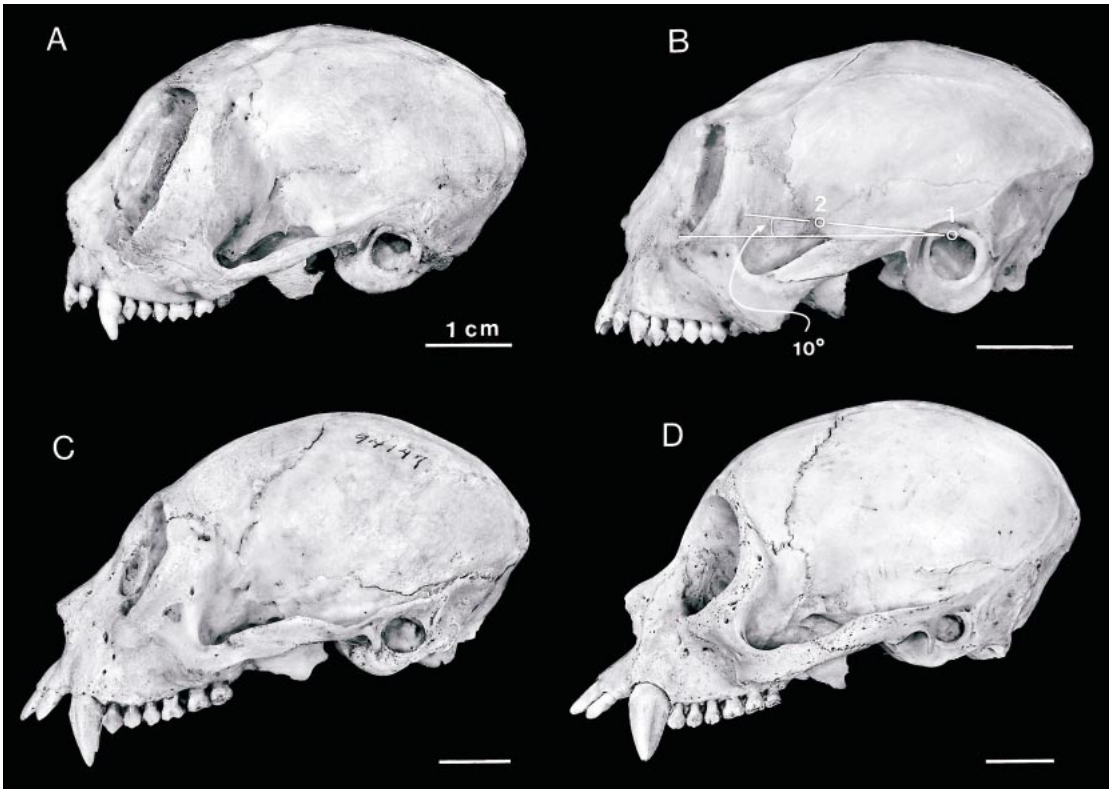

Fig. 14. Skulls of comparative set in modified Frankfurt plane (see text), left lateral view: (**A**) *Aotus azarae* AMNHM 211463, (**B**) *Callicebus cupreus* AMNHM 34636, (**C**) *Pithecia pithecia* AMNHM 94133, and (**D**) *Cacajao calvus* AMNHM 73720. In panel B, superimposed angle illustrates parietal measurement (see ch. 85, appendix 2): *1*, inner surface of dorsal rim of external acoustic meatus; *2*, anteroinferiormost point on parietal.

tally. This feature is present but less marked in *Paralouatta* and *Antillothrix* (cf. illustrations in Horovitz and MacPhee [1999] and MacPhee and Horovitz [2002]). In other pitheciids the two principal buccal cusps are mesiodistally aligned and similar in size (fig. 12B–D).

M2 is reduced distally, with the hypocone and metacone being barely distinguishable as separate cusps. The paracone is the best defined feature on the tooth, and like the M1 protocone, presents a prominent buccal bulge. The protocone area is slightly raised and worn flat. Each molar has three roots, two buccal and one lingual (fig. 11A, B).

PM3 and PM4 are bicuspid and almost identical morphologically, although PM3 is slightly smaller overall. In both specimens (figs. 9A, C; 11B, C), paracone and protocone are heavily worn; with difficulty mesial and distal parastyles can be discriminated on either side of the paracone. PM3 and PM4 possess two roots; PM2, represented by its alveolus only, seems to have had only one root.

Although canine crowns of *Xenothrix* remain unknown, root sizes can be accurately gauged from alveolar dimensions. As may be seen in table 6, BL and MD measurements of alveolar orifices of the pm2 and PM2 (= maximum inside dimensions of opening) are similar to those of the canine alveoli in the same jaws. (This character is to be distinguished from ch. 37, appendix 1, which compares the size of the fourth premolar's alveolar orifice to that of the canine.)

Greater discrimination can be gained by multiplying BL and MD measurements by AD (root length) in order to generate a volume modulus as a proxy for PM2/pm2 and C1/c1 root size. As may be seen in table 6, at least for the two specimens of *Xenothrix* that could be measured adequately, the root volume modulus for C1 is about 30% larger than that for c1. This is to be expected, as the usual condition in platyrrhines is one in which the maxillary canine is appreciably larger than the mandibular. However, the size relationship of the premolars is the reverse: pm2 root volume is about 20% larger than that of PM2. The same situation obtains in the comparative set, indicating that this relationship of premolar to root size is probably primitive.

Alveolar data cannot be used directly to infer whether the crowns of the canines projected past the occlusal level of adjacent teeth in *Xenothrix,* although on the basis of conditions in platyrrhines generally and in pitheciids specifically we consider this probable (figs. 6, 8, 14). At the same time, the degree of projection was probably quite small, along the lines seen in extant *Callicebus* and *Aotus* rather than *Pithecia* or any of the larger pitheciines (or other ceboids and ateloids generally). Inspection of a range of skulls of extant pitheciines lacking anterior teeth indicates that the C1 socket is typically about two to three times deeper than that of PM2. By contrast, if AMNHM 268006 is representative, in *Xenothrix* (table 6) the upper canine socket is only about 60% longer than that of the anterior premolar. In AMNHM 268001, c1 and pm2 roots are subequal.

Although within the comparative set only *Aotus* (fig. 13A) has truly spatulate upper incisor crowns, in owl monkeys as well as pitheciids I1 crowns are larger than those of the I2s (fig. 13B–D). In AMNHM 268006 there is no question that I1 roots were more substantial than those of I2s, but there is no independent evidence that the crowns were spatulate (see Discussion).

Living ceboids (which include *Aotus* in our view) differ from ateloids in that the former rely to a much greater degree on insects (Horovitz and Meyer, 1997). The known morphology of *Xenothrix* is consistent with the view that this monkey was mainly herbivorous, like the other members of its clade. In this connection it is interesting that *Xenothrix* evidently lacked substantial midfacial prognathism, large canines/diastemata, and highly procumbent lower incisors—all features of larger extant Pitheciinae. Without these specializations, the feeding maneuvers of *Xenothrix* doubtless differed from those of pitheciine ''sclerocarp foragers'' as described in detail by Kinzey (1992) and Rosenberger (1992). In sum, the dental evidence suggests that *Xenothrix* was a rather unspecialized frugivore, probably not unlike its closest living relative, *Callicebus*.

DISCUSSION: ORBITAL HYPERTROPHY, SPATULATE INCISORS, AND THE *AOTUS* HYPOTHESIS

In this section we focus on issues in craniodental morphological assessment raised by Rosenberger's (2002) *Aotus* hypothesis, or the argument that *Aotus*, not *Callicebus*, is the sister group of *Xenothrix*. This is necessary in any event because the definition and scoring of several of the characters used in the phylogenetic analysis in the next section are directly dependent on the accuracy of his assessments.

As outlined in the Introduction, Rosenberger's long-standing view is that *Xenothrix*, *Callicebus*, and *Aotus* are related as pitheciines (pitheciids in our taxonomy) because they share several derived features, among which are small canines and a deep jaw. To resolve their closer affinities, however, Rosenberger (2002) has recently emphasized the significance of two features which he identifies as ''high weight'' apomorphies—(1) enlarged orbits and (2) large, spatulate I1s. These features, he claimed, occur in *Aotus* and *Xenothrix* but not in *Callicebus*, thus settling in his opinion the question of sister-group relationships. We note in passing that, as Rosenberger's methodology is not based on parsimony analysis, he does not mention or even consider the possibility that one might find countervailing ''high weight'' apomorphies that uniquely link *Callicebus* and *Xenothrix* and the other Antillean monkeys. Be that as it may, the issue here is

whether the morphological evidence for orbit size and central incisors in *Xenothrix* has been correctly interpreted.

Size and Constitution of Bony Orbit

On the basis of conditions in AMNHM 268006, Rosenberger (2002: 157) claimed that the orbital morphology of *Xenothrix* resembled that of *Aotus* ''in all important respects''. In particular, Rosenberger pointed to (1) the *Aotus*-like condition of the IOF and (2) the ''wide arc'' described by the right orbital sill in this specimen, which he took to be evidence of ocular hypertrophy. Inspection of the views comprising figure 9 shows that there is virtually nothing left of the floor or sill of either orbit. Therefore, the degree to which they can be described as *Aotus*-like cannot be inferred merely from casual inspection. Nevertheless, Rosenberger's interpretations of *Xenothrix* could be of great significance if correct, because a widely dehiscent IOF and large orbit are derived traits of *Aotus* that contrast sharply with conditions in *Callicebus* (and indeed all other pitheciids). To evaluate this possibility we examined several morphological indicators which might be expected to provide some reliable information on the size and constitution of the bony orbit, even in a skull as damaged as AMNHM 268006. (Although we shall use the conventional terminology, we note that in platyrrhines it is often not meaningful morphologically to distinguish the superior orbital fissure as an entity distinct from the spheno-orbital foramen. The inferior orbital fissure, however, is always well marked even when nearly closed over.)

Construction of the Inferior Orbital Fissure

As a first approximation it could be argued that a widely dehiscent IOF is characteristic of primates with the largest eyes, but within-group variation in strepsirhines is actually rather inconsistent for this feature (Cartmill, 1980). Among extant haplorhines, *Tarsius* and (to a lesser extent) *Aotus* have large IOFs, which of course leads to the supposition that this feature may in fact be correlated with ocular hypertrophy in this group.

The IOF is usually treated as a single anatomical entity, but because it is a gap rather than a structure this approach may obscure more than it reveals. For morphological purposes we find it convenient to divide the inferior orbital fissure into anterolateral (AIOF) and posteromedial (PIOF) sections (figs. 15, 16). In platyrrhines the AIOF is defined by the orbital surfaces of the maxilla and zygomatic which grow together in various complex ways, ranging from widely open (as in *Aotus*; figs. 15A, 16A; table 7) to almost completely obliterated due to the approximation of bone territories (as in most *Callicebus*; figs. 15B, 16B; table 7).

In pitheciids generally (fig. 15B–D), zygomatic/maxillary contact tends to be broad: these two bone territories often grow together in such a way that the anteriormost part of the AIOF is pinched off as a separate foramen or slit, here identified as foramen innominatum.[6] In *Aotus*, the orbital surfaces of the zygomatic and maxillary are oriented differently than in pitheciids because of the laterad bulging of the orbits (figs. 13A, 15A). There is a significant gap between these bone territories not only medially but also laterally, where the lateral part of the AIOF yawns especially widely because the zygomatic's orbital surface is pushed out, as it were, onto the root of the zygomatic process. There is no question of a narrowly confined foramen innominatum being formed under these circumstances.

The PIOF is ventrally defined by the or-

[6] What this foramen transmits is uncertain, although by default the likeliest candidate on the basis of conditions in *Homo* (cf. Warwick and Williams, 1978) is a venous branch communicating between the ophthalmic v. and pterygoid venous plexus (of the external jugular v.). It is unlikely to be the infraorbital artery of the maxillary a., which normally enters through the posterior part of the IOF to course along with the infraorbital neurovascular bundle (cf. Bugge, 1974; Warwick and Williams, 1978). A separate orbital foramen for this vessel has never been reported for primates. Nor can the foramen represent an aperture for branches of the zygomatic nerve, as these originate within the orbit and run out through foramina (zygomaticofacial and zygomaticotemporal) located elsewhere. A brief survey of Old Word anthropoids indicates that the foramen (although not necessarily the vessel) is absent in catarrhines. Even in platyrrhine taxa in which the foramen is normally complete there may only be a notch or widened slit in the expected location. Here we shall simply identify the feature as a foramen innominatum (for examples, see figs. 15 and 16).

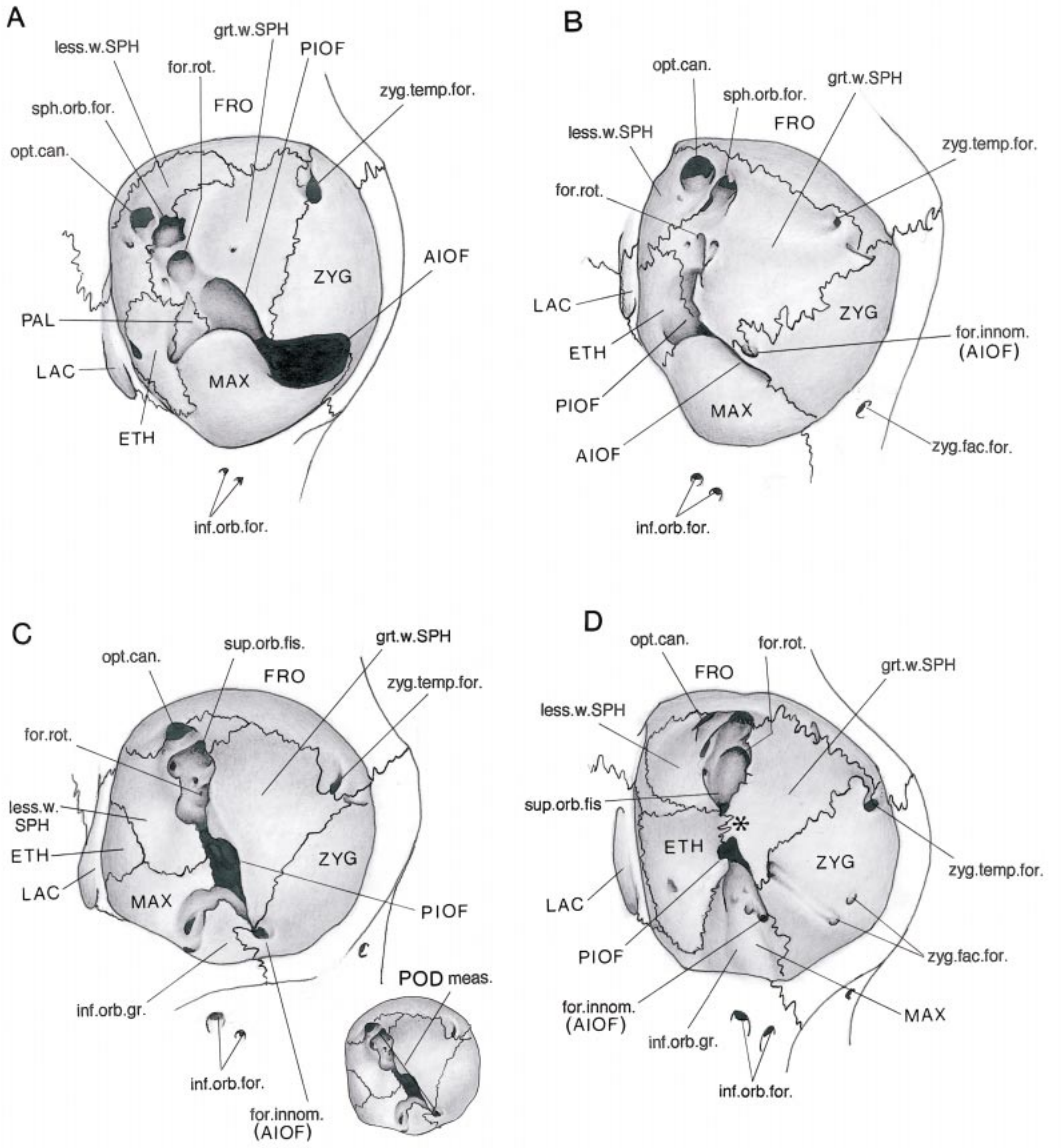

Fig. 15. Skulls of comparative set, left orbital mosaic (slightly schematic): (**A**) *Aotus*, (**B**) *Callicebus*, (**C**) *Pithecia*, and (**D**) *Cacajao*. Arrow in panel A illustrates measurement points for AIOF character (see ch. 87, appendix 2). *, roof over part of IOF formed by medial expansion of greater wing of sphenoid. Inset in panel C illustrates POD measurement (double-headed arrow; see text).

bital surface of the maxilla and the terminal part of the maxillary tuberosity and dorsally by the lower margins of the the sphenoid wings, where the gap grades insensibly into the superior orbital fissure. In contrast to the AIOF, in most platyrrhines the PIOF tends to remain widely open, and opposing bone territories either never grow together or do so only locally. For example, in large-bodied pitheciines a small tongue of bone, usually derived from the zygomatic or sphenoid, is often seen to roof over the proximal part of the channel for the infraorbital neurovascular bundle in carefully cleaned specimens (aster-

isk, fig. 15D). In other specimens the tongue seems not to have formed or to have been broken off during preparation.

In a general way IOF size in adult pitheciids seems to be correlated with body size: *Callicebus* has relatively and absolutely the narrowest IOF, while *Pithecia*, *Chiropotes*, and *Cacajao* display progressively wider gaps (ignoring the tongue just described). This correlation obviously does not hold for *Aotus* (fig. 15A): despite this monkey's comparatively small body size, both AIOF and PIOF are very wide and the contribution of the zygomatic to the lateral wall of the orbit is relatively slim. This suggests that conditions in the owl monkey are directed by factors other than those controlling degree of closure in pitheciids.

Turning now to the partial skull AMNHM 268006, it is evident that, while no detailed reconstruction of the IOF is possible, it is clear nevertheless that conditions are not at all *Aotus*-like. First, although most of the orbital wing of the zygomatic is not represented, the remaining part is in sutural union with the maxilla in the orbital floor. Zygomaticomaxillary contact does not occur in the floors of extant *Aotus* in the region of the IOF. Secondly, in the fossil the trailing margin of the zygomatic wing defines a notch (figs. 9D, 16E), which by virtue of its position must be the anterior end of the AIOF, in agreement with conditions not only in pitheciids like *Cacajao* (fig. 16D) but also in all other platyrrhines we have examined. The importance of this observation may be appreciated by imagining what the orbital skeleton of an owl monkey would look like if the zygomatic wing were broken away along the margin of the AIOF. Since there is no contact with the maxilla in this region, it follows that *no part of the zygomatic would be represented in the orbital floor* except anteriorly, where by necessity the zygomatic meets the maxilla to complete the postorbital plate and orbital sill. Since zygomatic material is unquestionably present in the fossil, pressed up against the lateral part of the maxillary tuberosity, this may be considered unequivocal evidence that the AIOF could not have been widely dehiscent as in modern *Aotus*.

A minor point that cannot be elucidated further without more complete remains is whether in *Xenothrix* the orbital wing of the zygomatic was typically reflected back onto the maxillary tuberosity, thereby creating a foramen innominatum. What is left of the orbital skeleton of *Xenothrix* does not preclude the possibility that the foramen was present, but nothing makes it particularly likely (or any more likely than the moderately open fissure seen in callitrichines, cebines, and large-bodied pitheciids). More positively, the morphology seen in *Alouatta*, *Brachyteles*, *Lagothrix*, *Ateles*, and *Paralouatta*, in which the anterior end of the AIOF is reduced to a very narrow slit, cannot have been present in *Xenothrix*.

In sum, the only thing that can be conclusively inferred about the AIOF in *Xenothrix* is that it must have been much narrower and differently shaped than in *Aotus*. Further, IOF size and shape are not necessarily coupled with orbit size: in *Paralouatta*, where orbit size is comparable to that of *Aotus*, the IOF nevertheless displays the narrow condition. We conclude from these considerations that Rosenberger's (2002) view that *Xenothrix* and *Aotus* are similar in IOF construction garners no support from comparative anatomy.

Estimating the Size of the Bony Orbit

Rosenberger (2002) asserted that enough remains of the orbital rim in AMNHM 268006 to permit a reasonable estimation of eyeball size, although he did not attempt to

→

Fig. 16. Skulls of comparative set, left inferior orbital fissure in oblique left lateral view (slightly schematic): (**A**) *Aotus*, (**B**) *Callicebus*, (**C**) *Pithecia*, (**D**) *Cacajao*, and (**E**) *Xenothrix* (AMNHM 268006). Foramen innominatum is not always complete (i.e., not entirely closed off from rest of inferior orbital fissure). AIOF is difficult to discriminate from PIOF in this view, so only the latter is specifically noted. Dashed line reconstructs probable shape of anterior terminus of AIOF in *Xenothrix*, which did not possess a wide AIOF like that of *Aotus* (A).

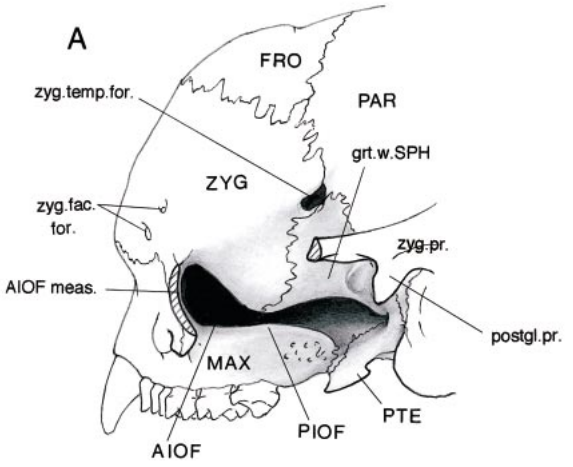

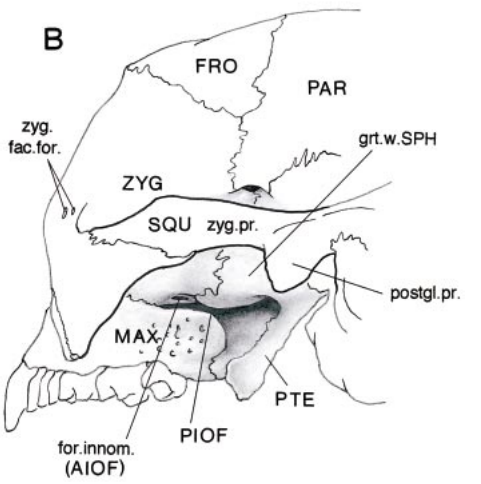

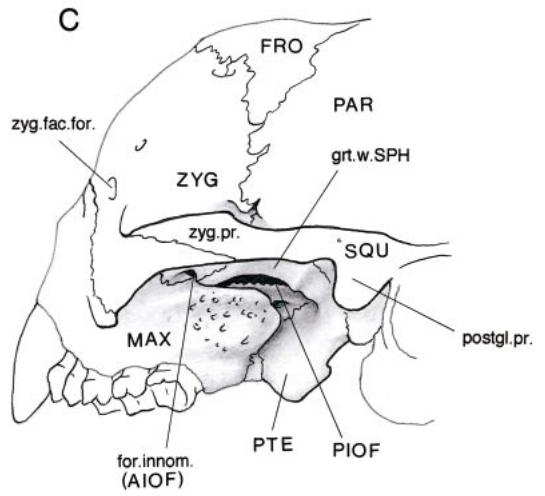

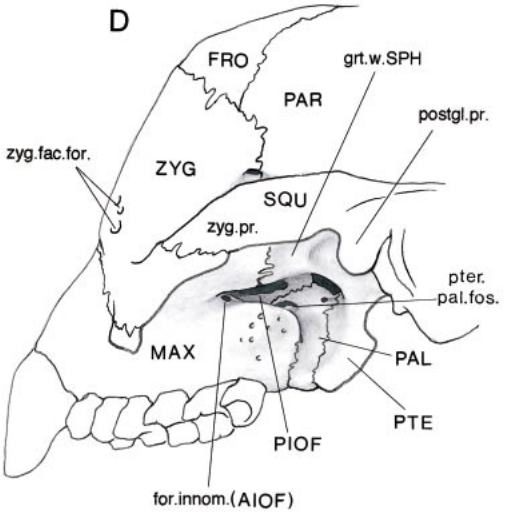

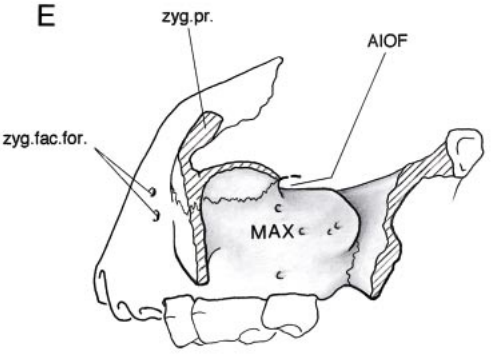

TABLE 7
***Xenothrix mcgregori* and Comparative Set: Anterior Portion of Inferior Orbital Fissure (IOF)[a]**

Taxon	Accession no.	Anterior IOF, width (mm) (I)	Maxillary tooth row, width at M1 loci (mm) (II)	Ratio I/II
Cebus olivaceus	AMNHM 100153	0.9	29.2	0.031
Saimiri sciureus	AMNHM 94098	1.0	17.5	0.057
Aotus azarae	AMNHM 211463	5.0	20.9	0.239
Callicebus caligatus	AMNHM 73705	1.0	20.6	0.049
Pithecia pithecia	AMNHM 79387	1.5	22.2	0.068
Cacajao calvus	AMNHM 76391	0.9	28.8	0.031
Chiropotes satanus	AMNHM 95867	0.6	22.1	0.027
Ateles belzebuth	AMNHM 76878	1.0	30.4	0.033
Lagothrix lagotricha	AMNHM 76042	0.2	30.7	0.007
Alouatta seniculus	AMNHM 140529	0.5	43.1	0.012
Brachyteles arachnoides	AMNHM 260	0.2	37.5	0.005
Callithrix argentata	AMNHM 95915	0.7	14.6	0.048
Saguinus bicolor	AMNHM 94096	1.2	18.3	0.066
Callimico goeldii	AMNHM 183290	0.5	17.4	0.023
Leontopithecus rosalia	AMNHM 70316	0.5	20.8	0.024
Xenothrix mcgregori	AMNHM 268006	1.0	26.1	0.038
Paralouatta varonai	MNHNCu V 194	0.2	36.2	0.005
Presbytis pileatus	AMNHM 43074	3.5	34.6	0.101
Hylobates lar	AMNHM 31593	3.5	30.6	0.114
Homo sapiens	Senior author's collection	7.5	59.4	0.126
Tarsius spectrum	AMNHM 196487	5.6	13.4	0.418

[a]For definition of this measurement, see character 87 (appendix 1) and text.

quantify this. In principle an empirically meaningful estimate of eyeball size in a fossil primate can be achieved by using a substitute, such as an appropriately shaped sphere of modeling clay. A model that is just large enough to pass through the orbital opening should be approximately equivalent to the size of the original eyeball (cf. MacPhee, 1987), although this makes no allowance for the intrinsic orbital muscles, fat, and other tissues that also fill the bony orbit (Schultz, 1940). Experience shows, however, that this method works well only if the bony orbit is complete or nearly so. If too little of the orbital rim and walls remain, then the diameter of the model cannot be adequately constrained and an erroneous (or, at any rate, an insecure) estimate of eyeball size may result. This is the case with AMNHM 268006: primate orbital rims are rarely perfectly circular, and a plausible arc of curvature cannot be derived from the few millimeters of rim that are still preserved on this specimen. In fact, the medioventral section of the orbital rim that is preserved in *Xenothrix* is typically almost straight in many platyrrhines (e.g., *Cebus*, *Callicebus*, *Saimiri*, *Pithecia*) and therefore independent of orbit size (cf. fig. 13B).

Utilization of Kay and Kirk's (2000) osteological method to derive information concerning activity pattern and visual acuity in extinct primates is also precluded, because none of the required variables (skull length, orbit diameter, optic foramen [canal] size) can be measured on AMNHM 268006. However, there is another method that can be applied in the present case. Although the foramina defined by the lesser wing of the sphenoid are no longer present in AMNHM 268006, the position of the medial wall of the optic canal can be reliably identified (see Description of New Specimens, Cranial Remains). Using this landmark as one terminus and the point at which the zygomaticomaxillary suture intersects the inferior margin of the orbit (internal wall) as the other, a proxy measurement for orbital depth (POD) can be taken (fig. 15C, inset). This measurement is related to, but is obviously not the same as,

true eyeball diameter. POD makes no allowance for eyeball sphericity, projection of the globe beyond the confines of the bony orbital margin, or distance between the orifice of the optic canal and the anatomical origin of the optic nerve on the eyeball. Our interest is simply to compare taxa (specimens) of varying body size for unit measurements that bear on the size of the bony orbit, in order to test whether or not *Xenothrix* had orbits of a size larger than expected.

Table 8 compares PODs and average body size (ABM) estimates for several platyrrhine taxa, including *Xenothrix*. POD is slightly smaller in *Xenothrix* than *Aotus*, but this is not especially meaningful in view of their substantial difference in body size. Rough adjustment for size can be achieved by dividing POD by ABM to generate an index, as is done in table 8 using natural log (ln) transformations. Results indicate that the orbits of *Xenothrix* are relatively small compared to those of other members of the comparative set, especially in the case of *Aotus*.

The same conclusion obtains when suitable allowance is made for the effect of allometry. As Schultz (1940) showed, there is a negative allometric relationship between eye size and body size in primates. This also applies to orbit size. Thus we should expect that, in proportion to body size, large primates will inevitably have smaller orbits than small primates do (cf. Kay and Kirk, 2000).

In the present case, performing an allometric correction is hindered by the fact that we lack body size estimates for specimens actually measured for POD (body size varies intraspecifically to a substantial degree within Platyrrhini [Ford and Corruccini, 1985]). Since appropriate data are unlikely to be gathered in the foreseeable future, any correction will have to be approximate. We utilized Schultz' (1940) data (which cover a much broader range of primate species than the set utilized here) to develop a linear regression expression relating orbital depth to body size. Derivation of the expression, in the form ln POD = 0.19(ln ABM) − 0.21, is explained in footnote e, table 8. It should be noted that all values in the last column of table 8 are much higher than 1 (expected ratio of left and right sides of the allometry equation), which probably reflects the introduction of various errors (original expression based on much wider sampling of primates, linear measurement indirectly derived from volumetric data, orbit depth and body weight not obtained from the same individuals/species). Although the dataset is therefore less clean than might be hoped, two general observations are warranted.

(1) With or without correction for allometry, *Xenothrix* falls close to taxa that have relatively small orbits as compared to *Aotus*. Indeed, *Aotus* stands apart from all other platyrrhines considered here: this is surely to be expected for a primate whose orbital index as defined by Martin (1990) places it in the top end of the range occupied by nocturnal lorises and lemurs. No matter how one wishes to express relative orbital size, *Xenothrix* emerges as different from *Aotus*—indeed, so different that they lie at opposite ends of the spectrum presented here.

(2) Accordingly, the bony orbits of the Jamaican monkey are not larger than expected, either in absolute terms or when compared with taxa in the same body size range. Instead, orbital depth appears to scale with measurements of other mid- to large-sized pitheciines, and not with *Aotus* (or *Callicebus*, for that matter). Even if one uses the lowest body weight (2 kg) that MacPhee and Fleagle (1991) considered reasonable for *Xenothrix*, the resulting index value is still only 2.5, comparable to *Pithecia* of average body size but quite unlike *Aotus*.

The case for *Aotus*-like orbital construction in *Xenothrix* thus founders. At least on the evidence considered here, Rosenberger's (2002) contention—that the Jamaican monkey followed the same ''adaptive trend'' that conditioned the evolution of orbital size in the owl monkey—appears to be without strong foundation.

INCISOR WIDTH

Rosenberger (2002: 157) argued that ''the first upper incisor alveolus is greatly enlarged in the fossil [i.e., AMNHM 268006], relative to the I2 socket. This is paralleled by a relatively large interalveolar distance separating right and left I1's. I interpret the morphology as an indication of a greatly broadened I1 crown, which is a novelty of *Aotus*.''

TABLE 8

***Xenothrix mcgregori* and Comparative Set: Orbital Depth/Body Size Index**

Representative species	ABM, male/female[a]	Midpoint ABM[b]	ln ABM	POD[c]	ln POD	ln POD/ ln ABM[d]	ln POD/ 0.19(ln ABM) − 0.21[e]
Aotus		988	6.895683	22.3 (21.3–23.5)	3.104587	0.45	2.82
trivirgatus	736/813						
azarae	1180/1230						
infulatus	1190/1240						
Callicebus		1150	7.047517	19.4 (18.5–20.7)	2.965273	0.42	2.63
cupreus	1020/1120						
moloch	960/1020						
torquatus	1210/1280						
Pithecia		2095	7.647309	22.7 (21.3–23.6)	3.122365	0.41	2.51
pithecia	1580/1940						
irrorata	2070/2250						
monachus	2110/2610						
Chiropotes		2865	7.960324	22.3 (21.5–23.5)	3.104587	0.39	2.38
satanas	2580/2900						
albinasus	2490/3150						
Cacajao		3020	8.013012	24.8 (23.4–25.5)	3.210844	0.40	2.45
calvus	2880/3450						
melanocephalus	2710/3160						
Xenothrix		3000	8.006368	21.3	3.058707	0.38	2.33
mcgregori	2000–4000						

[a]ABM, adult body mass (in grams), mean, for representative species as listed for each genus, expressed as male/female means (abstracted from relevant tables published by Fleagle, 1999). Notice that in some platyrrhine species males are smaller on average than females. Much lower average body sizes have been reported in the literature for some species (e.g., 450 g for *A. trivirgatus* by Ford and Corruccini, 1985), but such outliers cannot be regarded as representative.

[b]Midpoint ABM, based on "average" of smallest and largest body weights for each genus as recorded in second column. ABM for *X. mcgregori* is based on estimates published by MacPhee and Fleagle (1991).

[c]POD, proxy orbital depth (see text; in mm), mean and range; $N = 3$/taxon (except *Xenothrix*). AMNHM accession numbers of specimens measured: *Aotus* 209916, 211463, 239851; *Callicebus* 73705, 75988, 130361; *Pithecia* 94211, 187972, 187984; *Chiropotes* 94127, 94160, 96339; *Cacajao* 73720, 98316, 98473; *Xenothrix mcgregori* 268006. Unfortunately, body weights were not recorded for these specimens at the time that they were collected.

[d] Values not corrected for allometry.

[e]Values corrected for allometry. Divisor based on regression expression derived as follows: Slope was obtained by calculating a linear dimension correlated with orbital volume as a function of body weight, using the data of Schultz (1940). Using a variety of primates (far wider than those utilized in this study), Schultz (1940) showed that orbital *volume* and body weight are related by a function of slope 0.56. We derived a linear dimension, "diameter", by considering the orbit to be a sphere and using the common formula for calculating the volume of a sphere ($^4/_3\pi r^3$) to solve for r (radius) and multiplying the result by 2. Parameters 0.19 and −0.21 were then calculated from a new function between corresponding diameter and body weights. An identical slope of 0.19 is obtained whether one uses the diameter of a sphere or the side of a cube as proxies for orbital volume, as a function of body weight. Correction for the y-intercept (−0.21) was calculated for a function involving the diameter of a sphere with volume equal to the orbit volume expected by the function (orbit volume/body weight) also reported by Schultz (1940), where the intercept was −1.21. Expected values for the last column should be ~1.0 for primates overall if the regression (and its parameters) were well adjusted to the sample of primates selected here, but as explained in the text this condition does not obtain. Results are therefore to be regarded as gross approximations. Nevertheless, they tend to show that *Xenothrix* lies among taxa having relatively small orbits when compared with *Aotus*, whether or not a correction is made for allometry.

TABLE 9

***Xenothrix mcgregori* and Comparative Set: Incisor Alveolar Row Width (IARW) (in mm)[a]**

Taxon[b]	Maxillary IARW	Mandibular IARW
Aotus	9.5 (9.3–9.9)	7.0 (6.7–7.3)
Callicebus	9.0 (8.3–9.4)	6.1 (5.7–6.3)
Pithecia	11.1 (9.7–11.8)	7.5 (7.7–7.6)
Chiropotes	11.4 (11.0–12.7)	8.3 (7.5–9.4)
Cacajao	13.5 (13.1–13.8)	9.6 (9.2–9.8)
Xenothrix		
AMNHM 148198	—	6.9*
AMNHM 268001	—	6.0*
AMNHM 268006	11.8	—

[a]IARW, incisor alveolar row width, measured as maximum distance between lateral margins of alveolar orifices of lateral incisors, mean and range. Measurements that could not be taken accurately because of damage to specimen are followed by an asterisk (*).

[b]*N*/taxon varies. AMNHM accession numbers of specimens measured: *Aotus* 209916, 211458, 211460, 211463, 211481, 239851; *Callicebus* 73705, 75988, 98102, 130361; *Pithecia* 79387, 94147, 94133 (skull only), 94211, 187984 (mandible only); *Chiropotes* 76889, 94126, 94160, 95867; *Cacajao* 73720, 76391, 98316, 98473.

TABLE 10

***Xenothrix mcgregori* and Comparative Set: Ratio of Areas of Alveolar Apertures of First and Second Maxillary Incisors**

Taxon[a]	Ratio, I1/I2 alveolar aperture areas[b]
Cebus	0.98 (0.85–1.08)
Saimiri	0.83 (0.71–0.92)
Aotus	0.56 (0.47–0.60)
Callicebus	0.62 (0.55–0.66)
Pithecia	0.77 (0.58–1.08)
Cacajao	0.59 (0.47–0.57)
Chiropotes	0.74 (0.58–0.82)
Xenothrix	0.63
Ateles	0.71 (0.54–0.79)
Lagothrix	0.87 (0.75–0.96)
Alouatta	1.10 (0.98–1.27)
Brachyteles	1.18 (0.86–1.18)
Callithrix	0.89 (0.75–1.00)
Saguinus	0.99 (0.81–1.22)
Callimico	0.95 (0.81–1.14)
Leontopithecus	0.75 (0.68–0.85)

[a]*N*/taxon varies. AMNHM accession numbers of specimens measured: *Callicebus* 73705, 75988, 130361; *Pithecia* 36321–36323, 76815; *Cacajao* 73720, 76391, 78565, 78568, 78569, 78571, 98316; *Chiropotes* 95872, 96340, 96343, 96344; *Xenothrix* 268006; *Ateles* 76896, 76897; *Lagothrix* 188153, 188154; *Brachyteles* 128, 260, 80405; *Callimico* 98281, 98367, 176602, 239601; *Leontopithecus* 3844, 70181. LACM accession numbers of specimens measured: *Cebus* 27326, 27327, 27343, 55233; *Saimiri* 27320, 27321, 27323, 27324; *Aotus* 27257–27259, 60645; *Callicebus* 90817; *Pithecia* 90818, 90819, 90821, 90822; *Cacajao* 27341; *Chiropotes* 27276–27279; *Ateles* 27358–27360; *Lagothrix* 90758, 90830; *Alouatta* 14382, 27352, 27354, 27358; *Callithrix* 89, 5489, 27298, 27298; *Saguinus* 27292, 27294, 27340, 31542; *Leontopithecus* 70212, 90759.

[b]Area defined as BL × MD. For definition of this measurement, see character 86 (appendix 1) and text.

In the absence of incisor teeth allocatable to *Xenothrix* it is fruitless to enter into an extended discussion of this topic, although some brief observations on alveolar dimensions are warranted. As already noted, the mere fact that the alveoli of the maxillary central incisors in AMNH 268006 are larger than those of the lateral incisors does not indicate that the crowns were *Aotus*-like in their shape or proportions. In this specimen the row width of maxillary incisor alveoli is only 11.8 mm (table 9), which is little different from the equivalent measurement in large-bodied pitheciines (cf. figs. 9C and 13C, D). Presumably, if the upper incisors of *Xenothrix* had been broad and shovel-shaped like those of *Aotus*, row width would have been disproportionately greater.

To investigate the relationship of I1/I2 alveoli further, we measured representatives of all platyrrhine genera (see table 10 and Phylogenetic Analysis). We found that having an I1 aperture much larger than that of I2 is not an exclusive characteristic of *Aotus* and *Xenothrix*: it also occurs in *Callicebus* and *Cacajao*. Also, *Pithecia*, *Chiropotes*, and *Ateles* show extensive overlap in values with these last-named taxa. Further, the separation of I1 alveoli is a highly variable feature, as is evident by inspection of any large group of humans. Even among *Aotus* specimens this feature is not consistent (cf. *Aotus lemurinus* LACM 27258, *A. lemurinus* LACM 27259, *A. azarae* LACM 60645, all of which display unremarkable separation of I1 alveoli). By contrast, broad separation of I1 alveoli occurs in many species, whether or not ''spatulate'' upper incisors are present and regardless of I1/I2 alveolar proportions (cf. *Callicebus* sp. LACM 90817; *Pithecia monachus* LACM 90818; *Pithecia pithecia* LACM

90822; *Chiropotes satanas* LACM 27276, 27277, 27279; *Cebus albifrons* LACM 56109, 30359; *Cebus apella* LACM 55233; *Saimiri sciureus* LACM 90823, 27322, 5488).

There is even less reason to think that the mandibular incisors of *Xenothrix* could have been shaped like those of *Aotus*. In the two fossil mandibles that can be measured for this feature, incisor alveolar row width (table 9) is extremely narrow, even after allowance is made for damage. We therefore disagree with Rosenberger (1977: 470) who, citing Williams and Koopman (1952), maintained that the lower incisors of *Xenothrix* could not have been as closely packed as in pitheciines. To be sure, average row width in *Aotus* is metrically similar to AMNHM 148198 and 268001, but the individual teeth (as judged by alveolar dimensions) are of course much smaller, reflecting greater root spacing to accommodate the spadelike, orthally implanted incisor crowns characteristic of owl monkeys.

Thus, although the fossil documentation is admittedly poor, there does not currently seem to be any persuasive evidence in favor of Rosenberger's argument that *Xenothrix* possessed spatulate incisor crowns resembling those of *Aotus*, while there is considerable circumstantial evidence against it. Although it is questionable whether incisor morphology in *Xenothrix* exactly replicated that of any living species, the few measurements that can be taken suggest that the mandibular incisor crowns in particular had to have been relatively slender, which is a primitive platyrrhine feature. If *Xenothrix* is still to be considered an aotine, it seemingly lacks an important apomorphy of that group.

PHYLOGENETIC ANALYSIS

Materials and Methods

In a previous paper (Horovitz and MacPhee, 1999), we conducted a cladistic study that included representatives of all living genera of platyrrhines and the fossil species *Paralouatta varonai*, *Xenothrix mcgregori*, *Antillothrix bernensis*, *Stirtonia victoriae*, and *S. tatacoensis*. That analysis utilized 80 characters and included the new specimens of *Xenothrix* described in this paper. Our results indicated that the Antillean species formed a monophyletic group, the sister taxon of which was *Callicebus*.

In this paper we reanalyze our original data in light of three additional characters newly coded for this analysis (see appendix 1, chs. 85–87), as well as six other characters that were coded by one of us in a previous paper (Horovitz, 1999). *Callithrix* has been shown to include *Cebuella pygmaea* (Canavez et al., 1999a, 1999b; Porter et al., 1997, 1999), so we eliminated *C. pygmaea* as a terminal taxon. Two characters exclusive to these two taxa (chs. 30 and 32 in Horovitz and MacPhee [1999] and Horovitz [1999]) were therefore deleted because they have become uninformative under the new arrangement. Thus the total number of characters now included in our analysis is 87. Among fossil taxa, *Tremacebus harringtoni* and *Nuciruptor rubricae* were added because of their putative relevance to the placement of *Xenothrix*. Scoring for these taxa is naturally limited to those characters for which there is empirical evidence. Outgroup taxa include *Tarsius*, a set of living catarrhines (including both cercopithecoids and hominoids), and the Oligocene Fayum anthropoid *Aegyptopithecus zeuxis*. When logically possible, multistate characters were ordered additively. Missing characters are scored as question marks and inapplicables as dashes, although operationally there is no difference between the two. Taxa with multiple entries for a character are coded as polymorphic.

As there is discussion in the literature regarding orbit size in *Tremacebus*, we need to explain briefly why this taxon has not been scored for ch. 11 (appendix 1). Both Rusconi (1933) and Hershkovitz (1974) concluded that, despite the poor condition of the type (and only) skull, there were sufficient grounds to infer that *Tremacebus* had enlarged orbits. Neither presented any measurements that might have served to substantiate their statements. However, Hershkovitz (1974: 10) also remarked that the orbits of *Tremacebus* were ''less expanded than in *Aotus*, more expanded than in *Callicebus*'' and thus somehow intermediate between these extremes. Fleagle and Rosenberger (1983: 144) thought that this representation was misleading: ''relative to the length of the

maxillary tooth row . . . the orbits of *Tremacebus* are only slightly larger than those of *Callicebus*, but considerably smaller than those of the nocturnal *Aotus*''. As already noted (see Discussion), in a more recent paper Rosenberger (2002: 157) has seemingly contradicted this presumably well-founded view, finding instead that ''the orbit of *Xenothrix* is enlarged, like [that of] *Aotus* and *Tremacebus*''. Like Hershkovitz' (1974) analysis, this statement was also made without benefit of supporting measurements. Because it is not apparent which, if any, of these relativistic, unquantified statements about orbit size in *Tremacebus* can be accepted, we coded the relevant cell as ''data missing''.

Character 85 is concerned with the extent to which the parietal participates in the pterion region of the external sidewall of the skull (see table 11). In atelids and pitheciids (including *Paralouatta*) the inferior edge of the parietal occupies a more ventral position in the pterion mosaic than it does in the other primates included in this analysis. We have attempted to quantify this difference (see fig. 19 and appendix 1). This region of the skull is not preserved in *Xenothrix*.

The remaining new characters concern aspects of platyrrhine morphology that have been adequately introduced in the preceding morphological sections of this paper, so we shall restrict our comments here to the matter of scoring. Character 86 concerns the relative size of the alveoli for I1 and I2 (see Discussion). Because we wanted to include *Xenothrix* in the analysis, we defined our character states on the basis of alveolar rather than crown measurements. Although the distribution of values was found to be essentially continuous and overlapping among platyrrhine genera (see table 10), in defining two states we were attempting to test Rosenberger's (2002) judgment regarding proportional differences between these teeth in *Aotus* as compared to other platyrrhines. Our results reveal that *Callicebus*, *Pithecia*, *Chiropotes*, *Cacajao*, *Ateles*, and *Leontopithecus* all display a level of difference between I1 and I2 that is equal to or greater than that encountered in *Xenothrix* or even some individuals of *Aotus*.

Our final character (ch. 87; see table 8) concerns the width of the anterior extremity of the infraorbital fissure (AIOF), with measurement performed as indicated in the character definition in appendix 1 and figure 16A. *Aotus* and *Tarsius* are outliers for this feature, having a very wide AIOF, whereas catarrhines show an AIOF slightly larger than that of most platyrrhines (the only exception being *Aotus*).

In addition to the foregoing, hypothetical characters with a scoring of ''1'' for *Aotus* and *Xenothrix* and of ''0'' for all other taxa were created to further test how this addition

TABLE 11
***Xenothrix mcgregori* and Comparative Set: Parietal Elevation Relative to Frankfurt Plane (in degrees)**

Taxon[a]	Parietal elevation[b]
Cebus olivaceus	19.0 (18–20)
Saimiri sciureus	18.7 (17–20)
Aotus azarae	28.3 (27–30)
Callicebus caligatus	10.7 (10–12)
Pithecia pithecia	9.7 (9–10)
Cacajao calvus	6.3 (5–7)
Chiropotes satanus	8.3 (7–11)
Ateles belzebuth	9.7 (7–12)
Lagothrix lagotricha	9.7 (7–13)
Alouatta seniculus	6.7 (4–9)
Brachyteles arachnoides	7.0 (5–9)
Callithrix argentata	18.7 (17–20)
Saguinus bicolor	14.0 (13–15)
Callimico goeldii	18.7 (15–22)
Leontopithecus rosalia	16.7 (16–17)
Paralouatta varonai	4.0
Presbytis pileatus	27.0
Hylobates lar	25.0
Homo sapiens	58.0
Tarsius spectrum	60.0

[a]Usually, $N = 3$/taxon (1/taxon if no range quoted). AMNHM accession numbers of specimens measured: *Cebus* 32058, 78494, 100153; *Saimiri* 42323, 64096, 94098; *Aotus* 209916, 211460, 211463; *Callicebus* 73705, 130361, 211460; *Pithecia* 76413, 79387, 94133; *Cacajao* 73720, 76391, 98316; *Chiropotes* 76889, 94160, 95867; *Ateles* 76878, 76882, 76883; *Lagothrix* 76042, 93713, 98357; *Alouatta* 48120, 140527, 142944; *Brachyteles* 128, 260, 80405; *Callithrix* 94933, 95915, 95921; *Saguinus* 37462, 94096, 94199; *Callimico* 98281, 183289, 183290; *Leontopithecus* 70181, 70316, 119470; *Presbytis* 43074; *Hylobates* 31593; *Homo* senior author's collection; *Tarsius spectrum* 196487. MNHNCu accession number of specimen measured: *Paralouatta* V 194.

[b]Parietal elevation, in degrees, mean and range. For definition of measurement, see character 85 (appendix 1) and text.

would affect the recovered phylogeny. One character was added at a time until a change in the topology of the phylogeny was produced. The goal behind this addition was to test how many characters exclusive for *Aotus* and *Xenothrix* would be needed before these two taxa appeared as sister groups.

A maximum parsimony analysis was performed using the program PAUP* (Phylogenetic Analysis Using Parsimony), version 4.0b10 (Swofford, 2002) applying a heuristic search with 100 replications. Wagner trees were obtained with random addition sequence of taxa, and they were subjected to TBR. *Tarsius* was the designated root of the trees.

We obtained Bremer support values for each branch (Bremer, 1988; Källersjö et al., 1992) and inspected strict consensus trees up to four steps longer than the most parsimonious trees (four separate trials, adding one step per trial). The program MacClade 4 (Maddison and Maddison, 2000) was used to change the position of *Aotus* and *Xenothrix* and to assess the number of steps needed to implement this change relative to the most parsimonious tree(s).

Results

Our data matrix is presented in appendix 2. The heuristic search yielded 9 MPTs, the strict consensus of which is shown in figure 17 (tree length = 293 steps; CI = 0.52, RI = 0.64, RC = 0.33). The resulting relationships (except for the addition of *Nuciruptor rubricae* and *Tremacebus harringtoni*) are identical to the ones published by Horovitz and MacPhee (1999). *Nuciruptor* appears as the sister group of *Cebupithecia* + Pithecinae, in agreement with Meldrum and Kay (1997) and Horovitz (1999). *Tremacebus* appears in a trichotomy nested within the Ceboidea, in general agreement with Horovitz (1999). However, the latter analysis included a host of other fossil taxa with which *Tremacebus* formed a group nested above *Cebus* and *Saimiri* and more basal than the Callitrichinae. The nine trees differ in regard to relationships detected among atelids (*Brachyteles*, *Ateles*, *Lagothrix*, and Alouattinae) and the relationships among *Tremacebus*, *Saimiri*, and the callitrichines. Decay values are low mainly because of the positional volatility of the fossil specimens included in the analysis: several of them have a very large number of missing entries and can fit anywhere in the tree within a low range of additional steps. A list of all unambiguous changes is shown in table 12. We note that the number of apomorphies for the two clades in which *Nuciruptor* and *Tremacebus* are placed is decreased compared to those reported by Horovitz and MacPhee (1999). This is due to the lack of information pertaining to many of those characters in these fossil taxa, which renders character optimizations ambiguous at relevant nodes.

The clade consisting of *Callicebus* and the Antillean species (node 42, fig. 17) is supported, as previously reported (Horovitz and MacPhee, 1999), by four unambiguous characters: (1) presence of two prominences on the lateral wall of the promontorium (ch. 15, derived from presence of a flat surface or presence of a single prominence); (2) presence of a zygomatic arch that extends ventrally below the level of the part of the alveolar process bearing the posterior cheekteeth (ch. 23, derived from a higher position of the zygomatic arch); (3) a mandibular canine root that is highly compressed (ch. 32, derived from a more rounded outline); and (4) C1 alveolar orifice (BL × MD) that is smaller than that of PM4 (ch. 60, derived from a C1 alveolar opening larger than that of PM4). As noted in the descriptive section, the utility of character 2 is compromised somewhat by the existence of size/sexual variation in the development of muscle origins on the underside of the zygomatic arch.

The Antillean clade resolves as: (*Xenothrix* (*Paralouatta*, *Antillothrix*)). It is supported by three unambiguous characters: (1) presence of a wide nasal fossa, wider than the palate at the level of M1 (ch. 25, derived from a narrower palate; see Horovitz and MacPhee, 1999: fig. 10); (2) buccolingually small c1 alveolar orifice compared to that of pm4 (ch. 37, derived from a c1 alveolus buccolingually wider than that of pm4); and (3) presence of a bulging buccal surface of the M1 protoconid (ch. 51, derived from absence of this feature).

Regarding the three new features included in this analysis, the relative size of alveoli

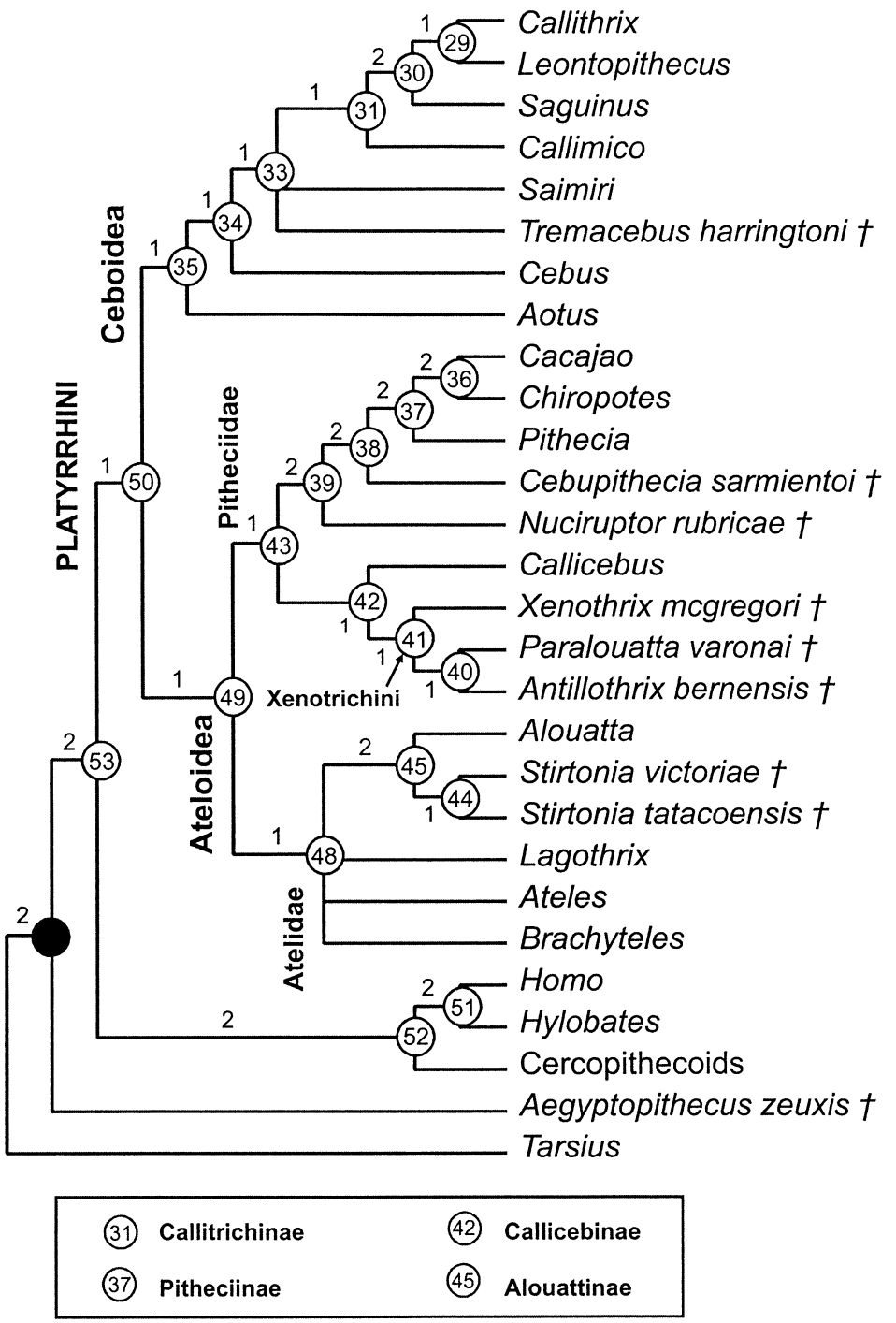

Fig. 17. Consensus tree of nine most parsimonious trees (87 morphological characters, TL = 293, CI = 0.52, RI = 0.64, RC = 0.33). Numbers in circles match node numbers in list of apomorphies (table 12). Numbers next to circles are Bremer support values (see Bremer, 1988). Daggers (†) identify fossil taxa.

TABLE 12
List of Apomorphies[a]

Node		Character	Change
53	45	Metaconid height on pm4	0 → 1
	46	Hypoconid pm4	0 → 1
	47	Entoconid on pm4	0 → 1
	53	m1/m2 buccal cingulum	1 → 0
	71	M1 postmetacrista slope	0 → 1
50	13	Tentorium cerebelli ossification	0 → 1
	17	Canal sigmoid sinus–subarc fossa	0 → 1
	24	Pterion region contacts	1 → 0
	76	M3 length	3 → 2
35	15	Middle ear paired prominences	0 → 1
	44	Metaconid height on pm3	1 → 2
	52	m1 entoconid position	1 → 0
	56	m3 length	3 → 2
	58	I1 lingual heel	1 → 0
	76	M3 length	2 → 1
34	56	m3 length	2 → 1
31	22	Cranial capacity	1 → 0
30	01	Offspring per birth	0 → 1
	16	Pterygoid fossa depth	0 → 1
	42	pm3 protoconid size	0 → 1
	56	m3 length	1 → 0
	70	M1 hypocone/prehypocrista	1 → 2
	74	M2 hypocone	1 → 0
	76	M3 length	1 → 0
29	14	Middle ear, pneumatization	0 → 1
	50	m1 cristid obliqua	1 → 0
49	16	Pterygoid fossa depth	0 → 1
	39	Deciduous pm2 cross section	1 → 0
	85	Parietal lower edge pterion region	0 → 1
43	54	m2 trigonid/talonid relative height	0 → 1
	70	M1 hypocone/prehypocrista	1 → 0
	86	Upper I2/I1 sockets	1 → 0
39	30	Permanent i1–i2 shape	0 → 1
	35	Lingual cingulum on c1 mesial elev	1 → 0
38	31	Diastema c1–i2	0 → 1
	34	Lingual crest on c1 sharpness	0 → 1
37	57	Molar enamel surface	0 → 1
	65	PM4 lingual cingulum	1 → 0
36	68	PM4 and M1 buccolingual breadth	0 → 1
	70	M1 hypocone/prehypocrista	0 → 1
42	15	Middle ear paired prominences	0 → 1
	23	Zygomatic arch, ventral	1 → 0
	32	Root c1 shape	0 → 1
	60	C1 alveolus size	0 → 1
41	25	Nasal fossa width	0 → 1
	37	c1 alveolus buccolingual breadth	0 → 1
	51	m1 protoconid buccal bulging	0 → 1
40	50	m1 cristid obliqua	0 → 1
	66	PM4 lingual cingulum mesial proj	0 → 1
	68	PM4 and M1 buccolingual breadth	0 → 1
	71	M1 postmetacrista slope	1 → 0
	72	M1 alignment protocone/hypocone	0 → 1
	73	M1 pericone/lingual cingulum	1 → 2
48	02	Lumbar vertebrae, number	0 → 1
	05	Tail, ventral glabrous surface	0 → 1
	20	Temporal emissary foramen	1 → 0
	64	PM4 protocone position	1 → 0
	65	PM4 lingual cingulum	1 → 0
47	40	pm2 size	0 → 1
	67	PM4 hypocone	0 → 1
	50	m1 intersect obl cristid/protolophid	0 → 1
	80	m1 buccolingual talonid width	0 → 1
44	77	Maxillary molar parastyles	0 → 1
46	44	Metaconid height on pm3	1 → 2
52	07	Carpometacarpal thumb joint	0 → 1
	12	Postglenoid foramen	1 → 0
	19	Ectotympanic shape	1 → 0
	65	PM4 lingual cingulum	1 → 0
51	04	External tail	1 → 0
	08	Ribcage shape	0 → 1
	09	Ulnar participation in wrist articulat	0 → 1
	10	Sternebral proportions	0 → 1

[a]Changes listed are those that appeared as unambiguous in all 9 MPTs.

for I1 and I2 (ch. 86) is large in both *Aotus* and *Xenothrix*, but this character state is also widespread among other platyrrhines. In MPTs, this character supports Pitheciidae (although with two reversals within terminals) and it appears independently in *Aotus*, *Ateles*, and *Leontopithecus*. The character state describing the wide AIOF (ch. 87) is an autapomorphy for *Aotus* and appears independently in *Tarsius* and (in an intermediate state) among catarrhines. Finally, the ventral extent of the parietal on the lateral wall of the skull (ch. 85) is an exclusive synapomorphy of Ateloidea. None of these characters contradicts the position of the Antillean species as sister group of *Callicebus*, and the last character further supports the hypothesis that Ateloidea does not include *Aotus*, as has been repeatedly shown with morphological and molecular data (see Horovitz [1999], Ho-

rovitz et al. [1998], and references cited therein).

Ten additional steps are needed to move *Aotus* from its most parsimonious position and place it as the sister group of *Xenothrix*, whereas seven steps are needed to remove *Xenothrix* from the Antillean clade and place it as the sister group of *Aotus* at the base of the Ceboidea. When hypothetical characters exclusively present in *Aotus* and *Xenothrix* were added to the analysis, four of them were needed before results began to change. With this option, some of the trees showed *Aotus* and *Xenothrix* together, whereas others still showed the same topology for the Antillean clade as the sister group of *Callicebus*. A fifth character would be needed to make *Xenothrix* and *Aotus* sister taxa in all shortest trees. In all cases in which *Xenothrix* appeared dissociated from the other Antillean taxa, it joined *Aotus* in the Ceboidea, and *Aotus* never appeared among the pitheciids.

CONCLUSION

The craniodental evidence we have treated in this and earlier papers supports three principal conclusions concerning the systematic position of *Xenothrix* (Horovitz and MacPhee, 1999; MacPhee and Horovitz, 2002): (1) *Xenothrix* is most closely related to extant pitheciids among living platyrrhines (and within that group, to *Callicebus*); (2) among extinct platyrrhines, *Xenothrix* groups with other Antillean primates; and (3) *Aotus* and *Xenothrix* display no uniquely derived characters in common. Candidate synapomorphies suggested by Rosenberger (2002), including enlarged orbits and spatulate upper incisors, either do not occur in *Xenothrix* or apply to a greater or lesser extent to a host of other platyrrhines. In short, there is no decisive evidence that would warrant placing *Xenothrix* next to *Aotus* to the exclusion of, or even in combination with, the members of family Pitheciidae. Exclusion of *Aotus* from close association with pitheciids is also supported by postcranial (Ford, 1986a), molecular (Schneider et al., 1993), and combined molecular and morphological evidence (Horovitz et al., 1998; Horovitz, 1999). Indeed, the molecular and combined molecular and morphological evidence suggests instead that owl monkeys are more closely related to the clade consisting of *Cebus*, *Saimiri*, *Tremacebus* (as shown in analyses involving morphology), and callitrichines than to any other platyrrhines (see also fig. 17).

MacPhee and Iturralde-Vinent (1995; Iturralde-Vinent and MacPhee, 1999) have argued on theoretical grounds that most lineages of Antillean land mammals (including the joint initiator of the Antillean monkey clade) were likely present on Caribbean landmasses by ~33 Ma. If this inference is correct, then the Antillean monkeys have a long and almost completely unknown history as an independent lineage. This point applies equally well to Pitheciidae in general, which seem to have undergone a prodigious radiation on the continent early in platyrrhine history—a radiation that is only spottily recorded in the existing fossil record (see Kay et al., 1998a). We are aware that a claim that pitheciids were in existence and had already differentiated into several subclades by the Early Oligocene is not in accord with the view that places the basal split in Platyrrhini (often incorrectly resolved as Callitrichinae vs. other platyrrhines) as late as 34–24 Ma (e.g., Purvis, 1995). Because molecular clocks are ultimately calibrated against the received fossil record, it is scarcely surprising that the origin of Platyrrhini is still relegated by many authors to the latest part of the Paleogene, which is when the empirical record begins in South America in the form of *Branisella boliviana*, a platyrrhine of uncertain relationships found in beds currently dated to Chron 8 (25.8–27.0 Ma) (Kay et al., 1998b; Fleagle and Tejedor, 2002). However, if the implications of the diversification model of Tavaré et al. (2002) are accepted, the last common ancestor of Primates could have lived no later than the latest Mesozoic (ca. 80 Ma), with the basal split between strepsirhines and haplorhines following shortly thereafter. Anthropoids were certainly in existence by the Early Eocene because their fossils have already been found (Beard and MacPhee, 1994; Beard, 2002). Yet if no more than 7% of all primates species that have ever lived have been recovered as fossils, as Tavaré et al. (2002) also claim, it is extremely unlikely that even the earliest anthropoids so far recognized are perched on or near the

actual point of the clade's origin. This argument applies a fortiori to the origin of Antillean monkeys (let alone platyrrhines), as it does, not so incidentally, to the origin and early radiation of caviomorph rodents (cf. Wyss et al., 1993). We continue to stand by our view that New World monkeys and rodents first entered the tectonically evolving insular Neotropics during the Oligocene from South America (Iturralde-Vinent and MacPhee, 1999), where their diversification must have already been well advanced (despite the absence of an empirical record to date).

No name has been assigned previously to the grouping of *Xenothrix*, *Paralouatta*, and *Antillothrix*. In view of the current taxonomic hierarchies in use for higher-level groups of platyrrhines, it is appropriate to assign the Antillean platyrrhine clade to **Xenotrichini** Hershkovitz (1970), new tribe. This tribe is the sister group of the monogeneric tribe Callicebini; these two tribes are in turn the constituents of Callicebinae, one of the two subfamilies of Pitheciidae. The ranking of this last clade was elevated from subfamily to family by Horovitz (1999: fig. 2B) to accommodate an increasing number of hierarchical levels due to new fossil discoveries. We hope that the new material explored in this paper reduces some of the mystery surrounding *Xenothrix*, the ''most enigmatic of all the South American extinct monkeys'' (Simons, 1972).

ACKNOWLEDGMENTS

It is a great pleasure to thank the colleagues and volunteers who have participated in our projects in Jamaica over the past decade. These include Lisa DeNault, Stephen Donovan, Adam Fincham, Alan Fincham, Clare Flemming, Ray Kielor, Greg Mayer, Don McFarlane, and Simon Mitchell. We also thank the Jackson's Bay Gun Club for permission to stay on its property and to Gun Club personnel Izzy and Makka. For illustrations we thank Lorraine Meeker and Patricia Wynne, assisted in various ways by Chester Tarka and Ruth O'Leary (all current AMNH personnel). Clare Flemming (The Explorers Club) read and improved an earlier version of this paper. Gary Morgan (New Mexico Museum of Natural History and Science), and John Fleagle and Chris Heesy (State University of New York, Stony Brook) reviewed our submitted text and caught several grievous errors and omissions. Permission to work in Jamaica was granted by the Natural Resource Conservation Department, Ministry of Mining, Government of Jamaica. Field investigations were partly supported by grants from the Adler Fund (to RDEM) and the National Geographic Society (to Don McFarlane).

REFERENCES

Beard, K.C. 2002. Basal anthropoids. *In* W.C. Hartwig (editor), The primate fossil record: 133–149. New York: Cambridge University Press.

Beard, K.C., and R.D.E. MacPhee. 1994. Cranial anatomy of *Shoshonius* and the antiquity of Anthropoidea. *In* J.G. Fleagle and R.F. Kay (editors), Anthropoid origins: 55–97. New York: Plenum Press.

Bremer, K. 1988. The limits of amino-acid sequence data in angiosperm phylogenetic reconstruction. Evolution 42: 795–803.

Bugge, J. 1974. The cephalic arterial system in insectivores, primates, rodents, and lagomorphs, with special reference to the systematic classification. Acta Anatomica 87(suppl. 62): 1–160.

Canavez, F.C., M.A.M. Moreira, J.J. Ladasky, A. Pissinatti, P. Parham, and H.N. Seuánez. 1999a. Molecular phylogeny of New World Primates (Platyrrhini) based on β_2-microglobulin DNA sequences. Molecular Phylogenetics and Evolution 12: 74–82.

Canavez, F.C., M.A.M. Moreira, F. Simon, P. Parham, and H.N. Seuánez. 1999b. Phylogenetic relationships of the Callitrichinae (Platyrrhini, Primates) based on β_2-microglobulin DNA sequences. American Journal of Primatology 48: 225–236.

Cartmill, M. 1980. Morphology, function, and evolution of the anthropoid postorbital septum. *In* R.L. Ciochon and A.B. Chiarelli (editors), Evolutionary biology of the New World monkeys and continental drift: 243–274. New York: Plenum Press.

Fincham, A. 1997. Jamaica underground, 2nd ed. Kingston: University of the West Indies.

Fleagle, J.G. 1999. Primate adaptation and evolution, 2nd ed. San Diego: Academic Press.

Fleagle, J.G., and A.L. Rosenberger. 1983. Cranial morphology of the earliest anthropoids. *In* M. Sakka (editor), Morphologie evolutive, mor-

phogenèse du crâne et origine de l'homme: 141–153. Paris: CNRS.

Fleagle, J.G., and M.F. Tejedor. 2002. Early platyrrhines of southern South America. *In* W.C. Hartwig (editor), The primate fossil record: 161–173. New York: Cambridge University Press.

Ford, S.M. 1986a. Systematics of the New World monkeys. *In* D.R. Swindler and J. Erwin (editors), Comparative primate biology, 1: Systematics, evolution and anatomy: 73–135. New York: Alan R. Liss.

Ford, S.M. 1986b. Subfossil platyrrhine tibia (Primates: Callitrichidae) from Hispaniola: a possible further example of island gigantism. American Journal of Physical Anthropology 70: 47–62.

Ford, S.M. 1990. Platyrrhine evolution in the West Indies. Journal of Human Evolution 19: 237–254.

Ford, S.M., and R.S. Corruccini. 1985. Intraspecific, interspecific, metabolic, and phylogenetic scaling in platyrrhine primates. *In* W.L. Jungers (editor), Size and scaling in primate biology: 401–436. New York: Plenum Press.

Ford, S.M., and G.S. Morgan. 1986. A new ceboid femur from the late Pleistocene of Jamaica. Journal of Vertebrate Paleontology 6: 281–289.

Ford, S.M., and G.S. Morgan. 1988. Earliest primate fossil from the West Indies. American Journal of Physical Anthropology 75: 209.

Hershkovitz, P. 1970. Notes on Tertiary platyrrhine monkeys and description of a new genus from the Late Miocene of Columbia. Folia Primatologica 13: 213–240.

Hershkovitz, P. 1974. A new genus of late Oligocene monkey (Cebidae, Platyrrhini) with notes on postorbital closure and platyrrhine evolution. Folia Primatologica 21: 1–35.

Hershkovitz, P. 1977. Living New World monkeys (Platyrrhini) with an introduction to Primates. Chicago: University of Chicago Press.

Horovitz, I. 1999. A phylogenetic study of living and fossil platyrrhines. American Museum Novitates 3269: 1–40.

Horovitz, I., and R.D.E. MacPhee. 1999. The Quaternary Cuban platyrrhine *Paralouatta varonai* and the origin of Antillean monkeys. Journal of Human Evolution 36: 33–68.

Horovitz, I., and A. Meyer. 1997. Evolutionary trends in the ecology of New World monkeys inferred from a combined phylogenetic analysis of nuclear, mitochondrial, and morphological data. *In* T.J. Givnish and K.J. Sytsma (editors), Molecular evolution and adaptive radiation: 189–224. New York: Cambridge University Press.

Horovitz, I., R.D.E. MacPhee, C. Flemming, and D.A. McFarlane. 1997. Cranial remains of *Xenothrix* and their bearing on the question of Antillean monkey origins. Journal of Vertebrate Paleontology 17(suppl.): 54A.

Horovitz, I., R. Zardoya, and A. Meyer. 1998. Platyrrhine systematics: simultaneous analysis of molecular and morphological data. American Journal of Physical Anthropology 106: 261–281.

Iturralde-Vinent, M.A., and R.D.E. MacPhee. 1999. Paleogeography of the Caribbean region: implications for Cenozoic biogeography. Bulletin of the American Museum of Natural History 238: 1–95.

Källersjö, M., J.S. Farris, A. Kluge, and C. Bult. 1992. Skewness and permutation. Cladistics 8: 275–287.

Kay, R.F. 1990. The phyletic relationships of extant and fossil Pitheciinae (Platyrrhini, Anthropoidea). Journal of Human Evolution 19: 175–208.

Kay, R.F., and M. Cartmill. 1977. Cranial morphology and adaptation of *Palaechthon nacimienti* and other Paromomyidae, with a description of a new genus and species. Journal of Human Evolution 6: 19–53.

Kay, R.F., and E.C. Kirk. 2000. Osteological evidence for the evolution of activity pattern and visual acuity in primates. American Journal of Physical Anthropology 113: 235–262.

Kay, R.F., D. Johnson, and D.J. Meldrum. 1998a. A new pitheciin primate from the middle Miocene of Argentina. American Journal of Physical Anthropology 45: 317–336.

Kay, R.F., B.J. MacFadden, R.H. Madden, H. Sandeman, and F. Anaya. 1998b. Revised age of the Salla Beds, Bolivia, and its bearing on the age of the Deseadan South American Land Mammal ''Age''. Journal of Vertebrate Paleontology 18: 189–199.

Kinzey, W.G. 1992. Dietary and dental adaptations in the Pitheciinae. American Journal of Physical Anthropology 88: 499–514.

MacPhee, R.D.E. 1984. Quaternary mammal localities and heptaxodontid rodents of Jamaica. American Museum Novitates 2803: 1–34.

MacPhee, R.D.E. 1987. Basicranial morphology and ontogeny of the extinct giant lemur *Megaladapis*. American Journal of Physical Anthropology 74: 333–355.

MacPhee, R.D.E. 1996. The Greater Antillean monkeys. Revista de Ciència 18: 13–32.

MacPhee, R.D.E. 1997. Vertebrate palaeontology of Jamaican caves. *In* A. Fincham (editor), Jamaica underground, 2nd ed: 47–56. Kingston, Jamaica: University of the West Indies.

MacPhee, R.D.E., and J.G. Fleagle. 1991. Post-

cranial remains of *Xenothrix mcgregori* (Primates, Xenotrichidae) and other Late Quaternary mammals from Long Mile Cave, Jamaica. *In* T.A. Griffiths and D. Klingener (editors), Contributions to mammalogy in honor of Karl F. Koopman, Bulletin of the American Museum of Natural History 206: 287–321.

MacPhee, R.D.E., and C. Flemming. 2003. A possible heptaxodontine and other caviidan rodents from the Late Quaternary of Jamaica. American Museum Novitates 3422: 1–42.

MacPhee, R.D.E., and I. Horovitz. 2002. Extinct Quaternary platyrrhines of the Greater Antilles and Brazil. *In* W.C. Hartwig (editor), The primate fossil record: 189–200. New York: Cambridge University Press.

MacPhee, R.D.E., and M.A. Iturralde-Vinent. 1995. Earliest monkey from Greater Antilles. Journal of Human Evolution 28: 197–200.

MacPhee, R.D.E., I. Horovitz, O. Arredondo, and O. Jiménez Vázquez. 1995. A new genus for the extinct Hispaniolan monkey *Saimiri bernensis* (Rímoli, 1977), with notes on its systematic position. American Museum Novitates 3134: 1–21.

Maddison, W.P., and D.R. Maddison. 2000. MacClade 4, program and documentation. Sunderland, MA: Sinauer Associates.

Maier, W. 1980. Nasal structures in Old World and New World primates. *In* R. Ciochon and A.B. Chiarelli (editors), Evolutionary biology of New World monkeys and continental drift: 219–239. New York: Plenum Press.

Martin, R.S. 1990. Primate origins and evolution: a phylogenetic reconstruction. Princeton, NJ: Princeton University Press.

McFarlane, D.A., J. Lundberg, and A.G. Fincham. 2002. A late Quaternary paleoecological record from caves of southern Jamaica, West Indies. Journal of Cave and Karst Studies 64: 117–125.

Meldrum, D.J., and R.F. Kay. 1997. *Nuciruptor rubricae*, a new pitheciin seed predator from the Miocene of Colombia. American Journal of Physical Anthropology 102: 407–427.

Porter, C.A., J. Czelusniak, H. Schneider, M.P.C. Schneider, I. Sampaio, and M. Goodman. 1997. Sequences of the primate ε-globin gene: implications for systematics of the marmosets and other New World primates. Gene 205: 59–71.

Porter, C.A., J. Czelusniak, H. Schneider, M.P.C. Schneider, I. Sampaio, and M. Goodman. 1999. Sequences from the 5′ flanking region of the ε-globin gene support the relationship of *Callicebus* with the pitheciins. American Journal of Primatology 48: 69–75.

Purvis, A. 1995. A composite estimate of primate phylogeny. Philosophical Transactions of the Royal Society, Biological Sciences 348: 405–421.

Rivero de la Calle, M., and O. Arredondo. 1991. *Paralouatta varonai*, a new Quaternary platyrrhine from Cuba. Journal of Human Evolution 21: 1–11.

Rose, K.D., and J.G. Fleagle. 1981. The fossil history of nonhuman primates in the Americas. *In* A.F. Coimbra-Filho and R.A. Mittermeier (editors), Ecology and behavior of Neotropical primates: 111–168. Rio de Janiero: Academia Brasileira de Ciencias.

Rosenberger, A.L. 1977. *Xenothrix* and ceboid phylogeny. Journal of Human Evolution 6: 461–481.

Rosenberger, A.L. 1992. Evolution of feeding niches in New World monkeys. American Journal of Physical Anthropology 88: 525–562.

Rosenberger, A.L. 2002. Platyrrhine paleontology and systematics: the paradigm shifts. *In* W.C. Hartwig (editor), The primate fossil record: 151–160. New York: Cambridge University Press.

Rosenberger, A.L., T. Setoguchi, and N. Shigehara. 1990. The fossil record of callitrichine primates. Journal of Human Evolution 19: 209–236.

Rusconi, C. 1933. Nuevos restos de monos fósiles del terciario antiguo de la Patagonia. Anales de la Sociedad de Ciencias de Argentina 116: 286–289.

Schneider, H., M. Schneider, I. Sampaio, M. Harada, M. Stanhope, J. Czelusniak, and M. Goodman. 1993. Molecular phylogeny of the New World monkeys (Platyrrhini, Primates). Molecular Phylogenetics and Evolution 2: 225–242.

Schultz, A.H. 1940. The size of the orbit and of the eye in primates. American Journal of Physical Anthropology 26: 389–408.

Silva, M., and J.A. Downing. 1995. CRC handbook of mammalian body masses. New York: CRC Press.

Simons, E. 1972. Primate evolution: an introduction to man's place in nature. New York: Macmillan.

Stallings, J.R., L. West, W. Hahn, and I. Gamarra. 1989. Primates and their relation to habitat in the Paraguayan Chaco. *In* K.H. Redford and J.F. Eisenberg (editors), Advances in Neotropical mammalogy: 425–441. Gainesville, FL: Sandhill Crane Press.

Swindler, D.R. 2002. Primate dentition: an introduction to the teeth of non-human primates. New York: Cambridge University Press.

Swofford, D.L. 2002. PAUP* Phylogenetic analysis using parsimony (*and other methods), version 4.0b8. Sunderland, MA: Sinauer Associates.

Tavaré, S., C.R. Marshall, O. Will, C. Soligo, and R.D. Martin. 2002. Using the fossil record to estimate the age of the last common ancestor of extant primates. Nature 416: 726–729.

Warwick, R., and P.L. Williams. 1978. Gray's anatomy, 35th British ed. Philadelphia: Saunders.

Williams, E.E., and K.F. Koopman. 1952. West Indian fossil monkeys. American Museum Novitates 1546: 1–16.

Wyss, A.R., J.J. Flynn, M.A. Norell, C.C Swisher, R. Charrier, M.J. Novacek, and M.C. McKenna. 1993. South America's earliest rodent and recognition of a new interval of mammalian evolution. Nature 365: 434–437.

APPENDIX 1

CHARACTER LIST

See Horovitz and MacPhee (1999) for references and discussion concerning chs. 1 through 77 and 84 (originally numbered 1–29, 31, 33–79, and 80), and Horovitz (1999) for chs. 78–83 (originally numbered 80–85). Characters that are multistate and nonadditive are noted; all others are additive.

1. Offspring per birth, number: 0 = one, 1 = two.
2. Lumbar vertebrae, number: 0 = more than five, 1 = five or fewer.
3. External thumb: 0 = absent or reduced, 1 = present.
4. External tail: 0 = absent (not projecting), 1 = present.
5. Tail, ventral glabrous surface: 0 = absent, 1 = present.
6. Claws on all manual and pedal digits except hallux: 0 = absent, 1 = present.
7. Carpometacarpal joint of thumb: 0 = nonsaddle, 1 = saddle.
8. Rib cage, shape: 0 = larger dorsoventrally, 1 = larger laterally.
9. Ulnar participation in wrist articulations: 0 = present, 1 = absent.
10. Sternebral proportions: 0 = manubrium shorter than 36% of corpus length, 1 = manubrium longer than 46% of corpus length.
11. Orbit size: 0 = smaller than 1.9, 1 = larger than 2.1.
12. Postglenoid foramen: 0 = absent, 1 = reduced, 2 = large.
13. Tentorium cerebelli, ossification: 0 = absent, 1 = present.
14. Middle ear, pneumatization of anteroventral region: 0 = absent, 1 = present.
15. Middle ear, paired prominences on cochlear housing: 0 = absent, 1= present.
16. Pterygoid fossa, depth: 0 = deep, 1 = shallow.
17. Canal connecting sigmoid sinus and subarcuate fossa: 0 = absent, 1 = present.
18. Vomer, exposure in orbit: 0 = absent, 1 = present.
19. Ectotympanic, shape (nonadditive): 0 = tube I, 1 = ring, 2 = tube II.
20. Temporal emissary foramen: 0 = present and large, 1 = small or absent.
21. Eyeball physically enclosed: 0 = absent, 1 = present.
22. Cranial capacity: 0 = less than 15 cm^3, 1 = more than 15 cm^3.
23. Zygomatic arch, ventral extent: 0 = below plane of alveolar border of posterior cheekteeth, 1 = above plane of border.
24. Pterion region, contacts: 0 = zygomatic-parietal, 1 = frontal-alisphenoid.
25. Nasal fossa width: 0 = narrower than palate at level of M1, 1 = wider.
26. Infraorbital foramen, vertical position relative to maxillary cheekteeth in Frankfurt plane: 0 = above interval between (or caudal to) M1 and PM4, 1 = above interval between PM4 and PM3, 2 = above (or rostral to) anteriormost premolar.
27. Zygomaticofacial foramen, size relative to maxillary M1 breadth: 0 = smaller, 1 = larger.
28. Deciduous i2, shape (nonadditive): 0 = bladelike, lingual heel absent, 1 = bladelike, lingual heel present, 2 = styliform, lingual heel absent.
29. Relative height of i1 to i2: 0 = i1 absent, 1 = i1 lower than i2, 2 = i1 and i2 subequal.
30. Permanent i1–i2, shape: 0 = spatulate, 1 = styliform.
31. Diastema between c1 and i2: 0 = absent, 1 = present.
32. Root of c1, shape: 0 = rounded/suboval, 1 = highly compressed.
33. Lingual cingulum on c1, completeness: 0 = complete, 1 = incomplete or absent.
34. Lingual crest on c1, sharpness: 0 = rounded, 1 = sharp.
35. Lingual cingulum on c1, mesial elevation of: 0 = not elevated, 1 = elevated.
36. Lingual cingulum on c1, forming spike on mesial edge of tooth: 0 = absent, 1 = present.
37. Buccolingual breadth of alveolus of c1,

compared to pm4: 0 = c1 larger than pm4, 1 = c1 smaller than pm4.
38. Deciduous pm2, angle subtended by distal portion of mesiodistal axis and postprotocristid: 0 = smaller than 45°, 1 = larger than 45°.
39. Deciduous pm2, cross-sectional shape: 0 = rounded, 1 = mesiodistally elongated.
40. Size of pm2, relative to pm3 and pm4: 0 = pm2 smallest in premolar series, 1 = pm2 not the smallest.
41. Deciduous pm3, metaconid: 0 = absent, 1 = present.
42. Protoconid of pm3, size relative to pm4 protoconid: 0 = pm3 and pm4 protoconids subequal, 1 = pm3 protoconid largest.
43. Talonid of pm3: 0 = larger than pm2 talonid, 1 = subequal to pm2 talonid.
44. Metaconid height of pm3, relative to protoconid height: 0 = metaconid absent, 1 = metaconid lower than protoconid, 2 = metaconid and protoconid subequal, 3 = metaconid taller than protoconid.
45. Metaconid of pm4, height relative to protoconid height: 0 = metaconid lower than protoconid, 1 = metaconid and protoconid subequal, 2 = metaconid taller than protoconid.
46. Hypoconid of pm4: 0 = absent, 1 = present.
47. Entoconid of pm4: 0 = absent, 1 = present.
48. Number of premolars: 0 = two, 1 = three.
49. m1 projection of distobuccal quadrant (DB complex): 0 = not projecting, 1 = projecting (crown sidewall hidden in occlusal view).
50. m1 intersection of oblique cristid and protolophid: 0 = intersects protolophid buccally, directly distal to apex of protoconid, 1 = intersects protolophid more lingually, distolingual to apex of protoconid.
51. m1 buccal bulging of protoconid: 0 = absent, 1 = present.
52. m1 entoconid position: 0 = on talonid corner, 1 = distally separated from talonid corner by sulcus.
53. m1/m2 buccal cingulum: 0 = absent, 1 = present.
54. m2 trigonid/talonid relative height: 0 = trigonid taller than talonid, 1 = subequal.
55. m2 mesoconid: 0 = absent, 1 = present.
56. m3/pm4 relative length: 0 = m3 absent, 1 = m3 shorter, 2 = subequal, 3 = m3 longer.
57. Molar enamel surface: 0 = smooth, 1 = crenulated.
58. I1 lingual heel: 0 = absent, 1 = present.
59. I2 orientation: 0 = vertical, 1 = proclivious.
60. C1 alveolus size relative to PM4 equivalent: 0 = C1 larger than PM4, 1 = C1 smaller or equal to PM4.
61. Deciduous PM2, trigon: 0 = absent, 1 = present.
62. Deciduous PM3, hypocone: 0 = absent, 1 = present.
63. PM3 preparacrista: 0 = absent or vestigial, 1 = present.
64. PM4 protocone position: 0 = mesial to widest point of trigon, 1 = on widest point.
65. PM4 lingual cingulum: 0 = absent, 1 = present.
66. PM4 lingual cingulum mesial projection: 0 = absent, 1 = present.
67. PM4 hypocone: 0 = absent, 1 = present.
68. PM4 and M1, relative buccolingual breadth: 0 = PM4 narrower than M1, 1 = PM4 subequal to or wider than M1.
69. M1 mesostyle/mesoloph (nonadditive): 0 = absent, 1 = mesostyle present, 2 = mesoloph present.
70. M1 hypocone/prehypocrista presence: 0 = hypocone and prehypocrista present, 1 = hypocone present and prehypocrista absent, 2 = hypocone and prehypocrista absent.
71. M1 postmetacrista slope: 0 = distobuccal slope, 1 = distal or distolingual slope.
72. M1 mesiodistal alignment of protocone and hypocone: 0 = parallel, 1 = hypocone lingual.
73. M1 pericone/lingual cingulum: 0 = absent, 1 = lingual cingulum only, 2 = distinct pericone on lingual cingulum.
74. M2 hypocone: 0 = absent, 1 = present.
75. M2 cristae on distal margin of trigon (nonadditive): 0 = cristae form distinct, continuous wall between protocone and metacone, 1 = cristae interrupted by small fossa or do not form distinct wall, 2 = cristae absent or differently organized.
76. M3/PM4 relative mesiodistal length: 0 = M3 absent, 1 = M3 shorter than PM4, 2 = M3 and PM4 subequal, 3 = M3 longer than PM4.
77. Maxillary molar parastyles: 0 = absent, 1 = present.
78. Buccolingual width of maxillary M3 compared to M1: 0 = M3 at least 0.67 of M1, 1 = M3 almost 0.5 of M1.
79. Buccolingual width of m1 talonid plus buccal cingulum compared to talonid alone: 0 = cingulum narrow, 1 = cingulum wide.
80. Mandibular molar m1 buccolingual talonid width relative to the trigonid: 0 = trigonid

is 0.8–1 times talonid, 1 = trigonid is 0.6–0.7 times talonid.

81. Vertical prominence on c1: 0 =absent, 1 = present.
82. Relationship of zygomatic arch with inferior orbital fissure: 0 = independent, 1 = zygomatic arch represents anterior limit of inferior orbital fissure.
83. Prominence on pm2 crown buccal wall: 0 = absent, 1 = present.
84. Ventral flexion of the skull (airorhynchy): 0 = absent, 1 = present.
85. Parietal lower edge in pterion region: 0 = high, 1 = low. This character is based on the dihedral angle between the modified Frankfurt plane (inferiormost point on orbital sill to the inner surface of the dorsal rim of the external auditory meatus) and an intersecting line drawn between the aforementioned rim and the parietal's anteroinferiormost point (which normally occurs at the triple junction of parietal, zygomatic, and greater wing of sphenoid, although other configurations are also found). The angle to be measured is taken at the point of intersection (demonstrated for *Callicebus* in fig. 14B). This can be easily accomplished with a microscope having a camera lucida attachment: the three required points (lowest point on orbit, inner rim of auditory meatus, lowest point on parietal) are indicated on tracing paper, lines are drawn through the origin (in this case the meatal rim), and a protractor is used to measure the arc. Note that because platyrrhines lack a tubular meatus, the Frankfurt plane as defined here is trivially different from the one defined in human osteology (meatal point is located slightly more laterally and ventrally in humans).
86. Relative size of alveoli for I1 and I2: 0 = alveolus for I2 much larger than alveolus for I1, 1 = alveoli subequal or the former slightly larger than the latter. Alveolar ''size'' is defined as the product of the mesiodistal and labiolingual dimensions of the alveolar aperture, and is therefore an estimator of alveolar aperture area. Two character states were implemented: ''0'' was scored for all individuals having an alveolar area index (I2/I1) of 0.66 or smaller (which includes *Aotus* and *Xenothrix*), while ''1'' was scored for individuals having an index larger than 0.66. *Pithecia*, *Ateles*, *Chiropotes*, and *Leontopithecus* displayed polymorphism (both categories represented in samples). All individuals of *Aotus*, *Callicebus*, *Cacajao*, and the single representative of *Xenothrix* were found to exhibit state ''0'', while all other genera exhibit ''1''.
87. Inferior orbital fissure, anterior width: 0 = small, 1 = intermediate, 2 = large. This character is scored by employing the index of the minimum distance across the AIOF (1 mm posterior to its rostralmost point) divided by palatal breath (at M1). The objective here is to capture the ''size'' of the AIOF by controlling for body size via the palatal breadth measurement. Because in most platyrrhines the rostralmost part of the AIOF is simply an ever-narrowing gap, any minimum distance measurement taken at the end of the fissure would be infinitely small. We therefore set the calipers slightly posterior to the fissure's terminus so that all entries would be real numbers (and all indices rational). In many platyrrhines the foramen innominatum (demonstrated in figs. 15 and 16) is properly the rostralmost part of the AIOF; in these cases the distance given in table 8 is the width of the foramen. Taxa with indicies between 0.005 and 0.068 were scored as ''0''; those between 0.101 and 0.126 as ''1''; and those between 0.24 and 0.42 as ''2''.

APPENDIX 2
DATA MATRIX
Notation used: ? = missing data, − = inapplicable character, a = (01), b = (12).

	1	11	21	31	41
Tarsius	0011000000	1200000020	0011010101	0010101010	0011000100
Leontopithecus	1011010000	0211111011	1010020120	0010110011	?101100100
Saguinus	1011010000	0210111011	1010020120	0010110011	010b100101
Callimico	0011010000	0a10101011	1010021120	0010110011	?002100111
Callithrix	1011010000	0211111011	1010020011	0100100011	0111000100
Aotus	0011000000	1210101011	1100020120	0010aa0111	1002ba1100
Cebus	0011000000	0210101111	0110020120	0000100111	1003211100
Cacajao	0011000000	0a10011011	0110020221	1011000100	1001111100
Pithecia	0011000000	0110111011	0110020221	101100010a	1001b11100
Chiropotes	0011000000	0a100a1011	0110020221	101100010a	1002111100
Saimiri	0011000000	02a0101110	0110020120	0010a100a1	100211110a
Alouatta	0111100000	0110011010	0110001110	0010100101	1001011111
Lagothrix	0111100000	0a10011010	0110011120	0010a00101	10021a1100
Brachyteles	0101100000	0110011010	0110011??0	0010100??0	?0011a1110
Callicebus	0011000000	0010111011	1100021120	0110100100	1001111100
Ateles	0101100000	001001a010	0110011120	0010100101	10021a0100
Homo	0010-01111	0001000001	0111?00120	0100--1???	???10a1000
Hylobates	0100-01111	0000000001	0111010120	0010100???	1??0111000
Cercopithecoids	0011001000	0000000001	0111000120	0010110???	1??0111010
Aegyptopithecus zeuxis	???1??0???	02?0000?1?	0111?00?20	0110100???	???0000000
Cebupithecia sarmientoi	??????????	?0100?1?1?	?????20???	10110?0???	?????10100
Paralouatta varonai	??????????	12?011?011	01?0101??0	0110101??0	?002111101
Antillothrix bernensis	??????????	??????????	??????????	??????????0	???????101
Xenothrix mcgregori	??????????	??????????	??0?11????	01????1??0	???????100
Stirtonia victoriae	??????????	??????????	??????????	??????????	???????1?1
Stirtonia tatacoensis	??????????	??????????	??????????	0010110??1	???1?01111
Tremacebus harringtoni	??????????	??????????	?1????2????	??????????	???????101
Nuciruptor rubricae	??????????	??????????	?????????1	001001???0	??0?011100

	51	61	71	81
Tarsius	0010030001	000?100002	0?10031010	02000?2
Leontopithecus	0010000000	1?001000a2	1?10001-00	00000a0
Saguinus	0010000000	10011000a2	0?10001-00	0000010
Callimico	0000010000	1?01100010	11110111-0	0000010
Callithrix	0010000000	00011000a2	0?10001-00	1000010
Aotus	0000020000	1001100000	10a10100-0	0100002
Cebus	0001010000	1011100101	10011100-0	1010010
Cacajao	0101121110	10110-a101	10111200-0	0010100
Pithecia	0101111110	10110-a000	10111300-0	00001a0
Chiropotes	0101121110	11110-a101	10111200-0	00001a0
Saimiri	0010010000	11011001a1	0021011010	a000010
Alouatta	0100030100	10000-a021	00a11300-1	0001110
Lagothrix	0100030100	10000-1001	10010300-0	00a0110
Brachyteles	0?00030?00	??000-0021	1001?2?0-0	0000110
Callicebus	0101030101	1001101000	10111200-0	0000100
Ateles	0100030100	10000-1001	10010200-0	00001a0
Homo	0101030a00	??010-0001	10a10300-0	?000011
Hylobates	0100030100	?0010-0001	10a10300-0	00000a1
Cercopithecoids	0100030110	?1010-0001	10a12310-0	00000a1
Aegyptopithecus zeuxis	0110030100	??011010a1	0011a31010	?000???
Cebupithecia sarmientoi	010??20?10	??1110?000	1011?11?-0	?0?????
Paralouatta varonai	1100030?1	??00110110	01210200-0	00011?0
Antillothrix bernensis	??????????0	???111?101	01211?1?-?	???????
Xenothrix mcgregori	1101100??1	??11100000	100??00?-0	?0???00
Stirtonia victoriae	??????????	?0000-1021	10111?1?-?	?0?????
Stirtonia tatacoensis	01000?0???	??000-1021	10111?1?-1	0?0????
Tremacebus harringtoni	0000??0???	??????????	?????????1	???0???
Nuciruptor rubricae	01010?0???	??????????	??????????	???????

APPENDIX 3

SPECIES-LEVEL TAXA UTILIZED FOR COMPARATIVE INVESTIGATIONS

American Museum of Natural History, Department of Mammalogy (AMNHM)

Tarsius spectrum 196487
Callithix argentata 94933, 95915, 95921
Saguinus bicolor 37462, 94096, 94199
Leontopithecus rosalia 3844, 70181, 70316, 119470
Callimico goeldii 98281, 98367, 176602, 183289, 183290, 239601
Cebus olivaceus 32058, 78494, 100153
Saimiri sciureus 42323, 64096, 94098
Aotus azarae 209916, 211458, 211460, 211463
Callicebus cupreus 34636, 75988, 98102, 130361; *Callicebus caligatus* 73705, 130361, 211460
Pithecia monachus 76413; *Pithecia pithecia* 36321–36323, 76815, 79387, 94133, 94147; *Pithecia* sp. 187984
Chiropotes satanus 76889, 94126–94128, 94160, 95867, 95872, 96340, 96343, 96344, 96339
Cacajao calvus 73720, 76391, 78565, 78568, 78571, 98316, 98473
Ateles belzebuth 76878, 76882, 76883, 76897, 95038, 95039, 95042
Brachyteles arachnoides 128, 260, 80405
Lagothrix lagotricha 76042, 93713, 98357, 188153, 188154
Alouatta seniculus 48120, 140527,140529, 142944
Presbytis pileatus 4307
Hylobates lar 31593
Homo sapiens (senior author's collection)

Los Angeles County Museum of Natural History, Department of Mammalogy (LACM)

Callithrix argentata 5489, 27299, 27298; *Callithrix* sp. 89
Saguinus midas 27292, 27294; *Saguinus oedipus* 27340; *Saguinus* sp. 31542
Leontopithecus rosalia 70212, 90759
Cebus albifrons 27326, 27327, 56109; *Cebus apella* 27343, 55233
Saimiri sciureus 5488, 27320–27324, 90823,
Aotus azarae 60645; *Aotus lemurinus* 27257–27259
Callicebus sp. 90817
Pithecia monachus 90818; *Pithecia pithecia* 90819, 90821, 90822
Chiropotes satanas 27276–27279
Cacajao calvus 27341
Ateles belzebuth 27358–27360
Lagothrix sp. 90758, 90830
Alouatta seniculus 14382, 27352, 27354, 27358

Museo Nacional de Historia Natural, La Habana (MNHNCu)

Paralouatta varonai V 194